Peer-reviewed version available at Math. Comput. Appl. 2017, 22, 44; doi:10.3390/mca22040044

The analysis of nonlinear vibrations of top tensioned cantilever pipes conveying pressurized steady two-phase flow under thermal loading

Adeshina Adegoke, Ayo Oyediran

Department of Mechanical Engineering, University of Lagos, Nigeria

Abstract

This paper studied the nonlinear vibrations of top tensioned cantilevered pipes conveying pressurized steady two-phase flow under thermal loading. The coupled axial and transverse governing partial differential equations of motion of the system were derived based on Hamilton's mechanics with the centreline assumed to be extensible. Multiple scale perturbation method was used to resolve the governing equations, which resulted to an analytical approach for assessing the natural frequency, mode shape and the nonlinear coupled axial and transverse steady state response of the pipe. The analytical assessment reveals that at some frequencies the system is uncoupled, while at some frequencies a 1:2 coupling exists between the axial and the transverse frequencies of the pipe. Nonlinear frequencies versus the amplitude displacement of the cantilever pipe conveying two-phase flow at super critical mixture velocity for the uncoupled scenario exhibit a nonlinear hardening behaviour, an increment in the void fractions of the two-phase flow resulted to a reduction in the pipe's transverse vibration frequencies and the coupled amplitude of the system. However, increasing the temperature difference, pressure and the presence of top tension were observed to increase the pipe's transverse vibration frequencies without a significant change in the coupled amplitude of the system.

Key words:

Hamilton's principle; Nonlinear vibration; Two-phase flow; Critical mixture velocity; Cantilever pipes; Perturbation method

1. Introduction

Two-phase flow is a common flow phenomenon in various industrial pipes; in nuclear heat exchangers, pipes in process plants, thermal plants, subsea oil and gas explorations and many more. However, in spite of the vast occurrences of two-phase flow in pipes, most of the existing publications on the flow induced vibrations of pipes conveying fluids focused on the fluidelastic instability of pipes conveying single phase flow. Miwa *et al*. [1] did an in-depth review of the extent of existing work on two-phase flow induced vibrations, stating that there exist very few researches on the instability behaviour of pipes due to internal two-phase flow. In the review, it was explained that internal two-phase flow induced vibration can be initiated by various hydrodynamic phenomena, depending on the geometrical configurations of the flow channels and operating conditions, gas-liquid two-phase flow may create vibrations with various modes of amplitude and frequency. Monette and Pettigrew [2] presents an excellent experimental work on the fluidelastic instability of flexible tubes subjected to two-phase flow which might be one of the premier paper on the dynamics of pipe and also reveals the relationship between the void fraction and the linear dynamics of the pipe for a two-phase liquid-gas flow. The early studies on the nonlinear dynamics of cantilevered pipes conveying single phase flow either studied only the transverse displacement of the pipe or considered the longitudinal displacement using the inextensible centerline assumptions [3-5]. However,

the pioneering work by Ghayesh *et al*. [6] studied the nonlinear dynamics of cantilevered extensible pipe conveying fluid, with equations of motions of the coupled transverse and longitudinal displacements derived using the Lagrange equations for system containing non material volumes and highlighted that conversely to inextensible pipe, an extensible pipe elongates in the axial direction as the flow velocity increases.

Luczko et al. [7] highlighted that the dynamic behaviour of continuous systems, such as beams, moving tapes or pipes with the flowing fluid is governed by non-linear partial differential equations with appropriate boundary and initial conditions. As highlighted by Païdoussis [8], the nonlinear problems of pipe conveying fluids cannot be resolved analytically, but recourse need to be taken to adopt specialized analytical method like perturbation techniques, numerical time difference methods or a combined analytical-numerical method. Some publications have adopted the direct Lagrangian discretization method (Galerkin method) to convert the partial differential equations (PDEs) to ordinary differential equations (ODE) and then resolve the resulting ODE's using numerical techniques, Modarres and Païdoussis [9], Wang et al. [10], Sinir [11], Ritto *et al*. [12], Chen et al. [13]. The usage of analytical methods like perturbation techniques is highly common with researchers working on nonlinear problems Nayfeh [14], Nayfeh [15], Kesimli *et al* [16], Oz and Boyaci [17] where the solution were sought for by an asymptotic expansion or by perturbing the original set of equations in terms of a small parameter which is either present in the equation or introduced artificially. Some researchers working on the fluidelastic instability of pipes conveying fluids have adopted this technique to resolve the nonlinear dynamics of the pipes, some of these are the works of Enz [18] on the simple supported straight pipe using perturbation analysis with multiple time-scaled method and comparison with measurements made by Coriolis flowmeters, the study on the transverse vibrations of tension pipes conveying fluid with time dependent velocity using the multiple scale perturbation technique by Oz and Pakdemirli. [19], the study on the analysis of nonlinear vibrations of a pipe conveying an ideal fluid by Sinir and Demir [20].

Most of these existing publications on the nonlinear dynamics of cantilevered pipe conveying fluid were focused on single phase flow resolving the governing equations using various methods as highlighted in the review of literature. However, profoundly among authors who adopted the perturbation approach is the study of the uncoupled problem, solving only the transverse vibrations independent of the axial vibration. To the best of our knowledge, a perturbation approach for the resolution of the coupled nonlinear dynamics of a top tensioned cantilevered pipes conveying pressurized two-phase flow under thermal loading is still a reserved topic with possible intriguing outcome. In this paper, the governing equation of motion for the nonlinear coupled axial and transverse vibration of cantilever pipe conveying two-phase flow is derived and resolved by imposing the method of multiple scales perturbation technique directly to the systems equations (direct-perturbation method).

1 Problem formulation and modelling

Considering a system of cantilever cylindrical pipe of length (L), having a cross-sectional area (A), mass per unit length (m_p) and flexural rigidity (EI), conveying multiphase flow, flowing parallel to the pipe's center line. The center line axis of the pipe in its undeformed state is assumed to overlap with the Y-axis and the cylinder is assumed to vibrate in the (Y, X) plane (see fig. 1). To derive the system's governing equations of motion, the following basic assumptions were made for the cylinder and the fluid: (i) the mean flow velocity is constant; (ii) the cylinder is slender, so that the Euler–Bernoulli beam theory is

Preprints (www.preprints.org) | NOT PEER-REVIEWED | Posted: 6 October 2017 doi:10.20944/preprints201710.0030.v1

Peer-reviewed version available at Math. Comput. Appl. 2017, 22, 44; doi:10.3390/mca22040044

applicable; (iii) although the deflections of the cylinder may be large, the strains are small; (iv) the cylinder centreline is extensible.

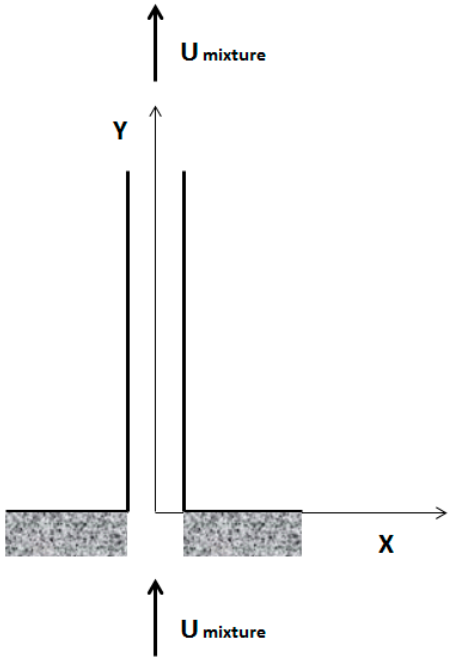

Figure 1: System's Schematics

The centreline of the cantilever pipe is assumed extensible to account for possible expansion due to the high temperature of the fluid content. The strain expressions and the geometric relation of the centreline of an extensible pipe are derived as expressed by Semler *et al* [3]:

1.1 Derivation of the Equation of Motion

The equations of motion are derived using the energy method. The energy method is based on the Hamilton's principle, which is defined as the variations of the time derivative of the Lagrangian. This can be mathematically expressed as:

$$\delta \int_{t1}^{t2} \mathcal{L}\, dt = \int_{t1}^{t2} \sum_{j=1}^{n} M_j U_j \left(\dot{r}_L + \sum_{j=1}^{n} U_j \tau_L \right) \delta r_L \; dt, \qquad (1)$$

Where

n is the number of phases in the fluid, which will be 2 for a two-phase flow

M_j is the mass of the phases in the fluid

U_j is the flow velocity of the phases in the fluid

$\mathcal{L}$ is the Lagrangian operator expressed in Eq. (2)

$$\mathcal{L} = \mathcal{T}_f + \mathcal{T}_p - \mathcal{V}_f - \mathcal{V}_p, \qquad (2)$$

Preprints (www.preprints.org) | NOT PEER-REVIEWED | Posted: 6 October 2017 doi:10.20944/preprints201710.0030.v1

Peer-reviewed version available at Math. Comput. Appl. 2017, 22, 44; doi:10.3390/mca22040044

$\mathcal{T}_p$ and $\mathcal{V}_p$ are the kinetic and potential energies of the pipe, and $\mathcal{T}_f$ and $\mathcal{V}_f$ are the kinetic and potential energies associated with the conveyed fluid.

The following expressions hold: $\dot{r}_L = \dot{u}_L i + \dot{v}_L k$ and $\tau_L = u'_L i + v'_L k$

1.1.1 Kinetic Energy

The total kinetic energy of the system is the summation of the kinetic energy of the pipe and the kinetic energies of the phases/components of the flowing fluid. The velocity vector of the pipe's centreline is expressed as:

$$\vec{V}_p = \frac{\partial u}{\partial t}\hat{\imath} + \frac{\partial v}{\partial t}\hat{\jmath} \tag{3}$$

Therefore, the kinetic energy of the pipe is expressed as:

$$\mathcal{T}_p = \frac{1}{2} m_p \int_0^L \left[\left(\frac{\partial u}{\partial t}\right)^2 + \left(\frac{\partial v}{\partial t}\right)^2\right] dx \tag{4}$$

As illustrated by Semler, the axial elongation of the pipe is complemented by a lateral contraction, due to the Poisson effect. This will impact the flow velocity of the fluid phases/components such that:

$$\sum_{j=1}^{n} U_j = [(1+\epsilon)/(1+a\epsilon)] \sum_{j=1}^{n} U_{0_j} \tag{5}$$

Where U_{0_j} and U_j are the flow velocities before and after elongation, the subscript (j) is used to identify the various phases/components of the conveyed fluid, (ϵ) is the axial strain and (a) relates to the Poisson ratio (v) as $a = 1 - 2v$; for an extreme case $v = 0.5$ and a becomes zero Ghayesh *et al* [6].

The flow velocity relative to the centerline axis of the pipe is expressed as:

$$\vec{V}_f = \left\{\frac{\partial u}{\partial t} + \sum_{j=1}^{n} U_j(1-a\epsilon)\left(1+\frac{\partial u}{\partial x}\right)\right\}\hat{\imath} + \left\{\frac{\partial v}{\partial t} + \sum_{j=1}^{n} U_j(1-a\epsilon)\left(\frac{\partial v}{\partial x}\right)\right\}\hat{\jmath} \tag{6}$$

Therefore, the Kinetic energy of the conveyed fluid is expressed as:

$$\mathcal{T}_f = \frac{1}{2}\sum_{j=1}^{n} M_j \int_0^L \left\{\left(\frac{\partial u}{\partial t}\right)^2 + \left(\frac{\partial v}{\partial t}\right)^2 + U_j{}^2\left[1 + 2\frac{\partial u}{\partial x} + \left(\frac{\partial u}{\partial x}\right)^2 - 2a\left(\frac{\partial u}{\partial x} + \frac{1}{2}\left(\frac{\partial v}{\partial x}\right)^2\right) + \left(\frac{\partial v}{\partial x}\right)^2\right] + 2U_j\left[\frac{\partial u}{\partial t}\left(1+\frac{\partial u}{\partial x}\right) + \frac{\partial v}{\partial t}\frac{\partial v}{\partial x}\right]\right\} dx \tag{7}$$

1.1.2 Potential Energy

Semler highlighted that the potential energy is as a result of the elastic deformation of the pipe and the effect of gravity and the deformation from elastic behavior of the pipe can be linked to the strain energy. This is expressed as:

$$\mathcal{V}_p = \frac{1}{2} EA \int_0^L \epsilon^2 dx + \frac{1}{2} EI \int_0^L (1+\epsilon)^2 k^2 dx \tag{8}$$

Preprints (www.preprints.org) | NOT PEER-REVIEWED | Posted: 6 October 2017 doi:10.20944/preprints201710.0030.v1

Peer-reviewed version available at Math. Comput. Appl. 2017, 22, 44; doi:10.3390/mca22040044

This is clearly the combinations of the axial strain effect and the bending strain effect where (E) denotes the Young's modulus, (I) denotes the pipe moment of inertia, (A) denotes the cross-sectional area, (ϵ) is the axial strain and (k) is the curvature term as expressed by Semler.

The thermal effect can be introduced by considering the linear strain tensor as a sum of the strain contributions from the mechanical stress and the thermal effect. Semler further decomposed the axial strain into a steady strain component due to externally applied tension (T_0) and pressure force component ($P = pA$) and an oscillatory strain component due to the oscillations of the pipe. These can be expressed as:

$$\epsilon_{ij} = \epsilon_{ij}{}^{\sigma} + \epsilon_{ij}{}^{\Delta} + \frac{T_0 - P}{EA} \tag{9}$$

While the stress contributing strain component is as expressed by Semler as:

$$\epsilon_{ij}{}^{\sigma} = \frac{\partial u}{\partial x} - \frac{1}{2}\left(\frac{\partial u}{\partial x}\right)\left(\frac{\partial v}{\partial x}\right)^2 + \frac{1}{2}\left(\frac{\partial v}{\partial x}\right)^2 - \frac{1}{8}\left(\frac{\partial v}{\partial x}\right)^4 \tag{10}$$

Considering that the gradient of the transverse displacement of the pipe is far greater than the gradient of the longitudinal displacement $\left(\frac{\partial v}{\partial x} > \frac{\partial u}{\partial x}\right)$. Also, the thermal contributing strain component can be expressed in terms of the thermal expansivity (α) and the difference in temperatures (ΔT) as

$$\epsilon_{ij}{}^{\Delta} = (-\alpha \Delta T) \tag{11}$$

Substituting Eq. (10) and Eq. (11) into Eq. (9) and then substituting Eq. (9) in to Eq. (8), the resulting expression is:

$$\mathcal{V}_p = \frac{1}{2}EA\int_0^L \left[\left(u' - \frac{1}{2}u'v'^2 + \frac{1}{2}v'^2 - \frac{1}{8}v'^4\right) + \frac{T_0 - P}{EA} + (-\alpha\Delta T)\right]^2 dx + \frac{1}{2}EI\int_0^L \left[v''^2 - 2v''^2u' - 2v''^2u''^2 - 2v'v''u''\right]dx \tag{12}$$

With the reference plane in the same direction as the gravitational acceleration, the effect of gravity can be expressed as:

$$\mathcal{V}_g = g\left(\sum_{j=1}^{n} M_j + m\right)\int_0^L (x + u)dx \tag{13}$$

The variations of the time derivative of the algebraic sum of the kinetic energy and the potential energy of the systems gives the expression on the left hand side term of the Hamilton's equation.

Preprints (www.preprints.org) | NOT PEER-REVIEWED | Posted: 6 October 2017 doi:10.20944/preprints201710.0030.v1

Peer-reviewed version available at Math. Comput. Appl. 2017, 22, 44; doi:10.3390/mca22040044

1.1.3 Non-conservative work done

As detailed by Semler for a single phase flow, the right hand side term of the Hamilton's can be expressed for a multiphase flow as:

$$\mathrm{EIv'''_L} = \sum_{\mathrm{j=1}}^{\mathrm{n}} \mathrm{M_j U^2_j} \int_{\mathrm{t1}}^{\mathrm{t2}} \mathrm{v'_L} \delta v \mathrm{dt} \qquad (14)$$

Physically, this implies a non-classical boundary condition at the free end for a discharging cantilever pipe. Therefore, a force is imposed at the free end if the velocity of the exiting fluid is not tangential to the pipe. However this study assumes that the exiting flow remains tangential to the pipe at the free end, therefore classical boundary condition holds at the free end.

1.2 Equation of motion for multiphase flow

The equation of motion for an extensible cantilever pipe conveying pressurized unsteady multiphase flow under thermal loading can be expressed as:

$$\left(m + \sum_{j=1}^{n} M_j\right)\ddot{u} + \sum_{j=1}^{n} \mathrm{M_j}\dot{U_j} + \sum_{j=1}^{n} 2M_j U_j \dot{u}' + \sum_{j=1}^{n} M_j {U_j}^2 u'' + \sum_{j=1}^{n} M_j \dot{U_j} u' - EAu'' - EI(v''''v' + v''v''')$$
$$+ (T_0 - P - EA(\alpha\Delta T) - EA)v'v'' - \left(T_0 - P - EA(\alpha\Delta T)\right)' + \left(m + \sum_{j=1}^{n} M_j\right) g = 0, \quad (15)$$

$$\left(m + \sum_{j=1}^{n} M_j\right)\ddot{v} + \sum_{j=1}^{n} 2M_j U_j \dot{v}' + \sum_{j=1}^{n} M_j {U_j}^2 v'' - \sum_{j=1}^{n} aM_j {U_j}^2 v'' + \sum_{j=1}^{n} M_j \dot{U_j} v' + EIv''''$$
$$- \left(T_0 - P - EA(\alpha\Delta T)\right)v'' - EI\left(3u'''v'' + 4v'''u'' + 2u'v'''' + 2{v'}^2 v'''' + 8v'v''v''' + 2{v''}^3\right)$$
$$+ (T_0 - P - EA(\alpha\Delta T) - EA)\left(u'v'' + v'u'' + \frac{3}{2}{v'}^2 v''\right) = 0 \qquad (16)$$

The associated boundary conditions are:

$$v(0) = v'(0) \; and \; v''(L) = v'''(L) = 0 \qquad (17)$$

$$u(0) = u'(L) = 0 \qquad (18)$$

1.2.1 Dimensionless equation of motion for multiphase flow

The equation of motion may be rendered dimensionless to make the analysis of the system more robust and not constrained to one specific system by introducing the following non-dimensional quantities;

$$\bar{u} = \frac{u}{L}, \quad \bar{v} = \frac{v}{L}, \quad \bar{t} = \left[\frac{EI}{\sum M_j + m}\right]^{1/2} \frac{t}{L^2}, \quad \bar{U}_j = \left[\frac{M_j}{EI}\right]^{1/2} UL, \quad \gamma = \frac{\sum M_j + m}{EI} L^3 g,$$

$$\beta_j = \frac{M_j}{\sum M_j + m}, \quad \Psi_j = \frac{M_j}{\sum M_j}, Damping\ term: \mu = \frac{CL^2}{\sqrt{\sum\left(M_j + m\right) EI}}$$

$$Tension: \Pi_0 = \frac{T_o L^2}{EI}, Flexibility: \Pi_1 = \frac{EAL^2}{EI}, Presure: \Pi_2 = \frac{PL^2}{EI}$$

Preprints (www.preprints.org) | NOT PEER-REVIEWED | Posted: 6 October 2017 doi:10.20944/preprints201710.0030.v1

Peer-reviewed version available at Math. Comput. Appl. 2017, 22, 44; doi:10.3390/mca22040044

$$\ddot{\bar{u}} + \sum_{j=1}^{n} \dot{\bar{U}}_j \sqrt{\Psi_j}\sqrt{\beta_j} + 2\sum_{j=1}^{n} \bar{U}_j \sqrt{\Psi_j}\sqrt{\beta_j}\dot{\bar{u}}' + \sum_{j=1}^{n} \Psi_j \bar{U}_j{}^2 \bar{u}'' + \sum_{j=1}^{n} \dot{\bar{U}}_j \sqrt{\Psi_j}\sqrt{\beta_j}\bar{u}' - \Pi_1 \bar{u}'' - (\bar{v}''''\bar{v}' + \bar{v}''\bar{v}''') + (\Pi_0 - \Pi_2 - \Pi_1(\alpha\Delta T) - \Pi_1)\bar{v}'\bar{v}'' - \left(\Pi_0 - \Pi_2 - \Pi_1(\alpha\Delta T)\right)' + \gamma = 0, \quad (19)$$

$$\ddot{\bar{v}} + 2\sum_{j=1}^{n} \bar{U}_j \sqrt{\Psi_j}\sqrt{\beta_j}\dot{\bar{v}}' + \sum_{j=1}^{n} \Psi_j \bar{U}_j{}^2 \bar{v}'' - a\sum_{j=1}^{n} \Psi_j \bar{U}_j{}^2 \bar{v}'' + \sum_{j=1}^{n} \dot{\bar{U}}_j \sqrt{\Psi_j}\sqrt{\beta_j}\bar{v}' - \left(\Pi_0 - \Pi_2 - \Pi_1(\alpha\Delta T)\right)v'' + \bar{v}'''' - \left(3\bar{u}'''\bar{v}'' + 4\bar{v}'''\bar{u}'' + 2\bar{u}'\bar{v}'''' + 2\bar{v}'^2\bar{v}'''' + 8\bar{v}'\bar{v}''\bar{v}''' + 2\bar{v}''^3\right) + (\Pi_0 - \Pi_2 - \Pi_1(\alpha\Delta T) - \Pi_1)\left(\bar{u}'\bar{v}'' + \bar{v}'\bar{u}'' + \frac{3}{2}\bar{v}'^2\bar{v}''\right) = 0 \quad (20)$$

The dimensionless boundary conditions are:

$$\bar{v}(0) = \bar{v}'(0) \; and \; \bar{v}''(L) = \bar{v}'''(L) = 0 \quad (21)$$

$$\bar{u}(0) = \bar{u}'(L) = 0 \quad (22)$$

In these equations, $\bar{u}$ *and* $\bar{v}$ are respectively, the dimensionless displacements in the longitudinal and transverse direction, $(\bar{U}_j)$ is the flow velocities of the constituent phases/components used in the parametric studies of the dynamics of the system, (β_j) is the mass ratio same as in single phase flows as derived by Semler and Paidoussis [8], (Ψ_j) is another mass ratio which is unique to multiphase flow relating the fluid mass independent of the mass of the pipe, (γ) is the gravity term and (Π_0, Π_1, Π_2) represent the Tension term, Flexibility term and the pressurization term respectively.

1.2.2 Dimensionless Equation of motion for two-phase Flow

The dimensionless governing equation can be reduced to that of a two-phase as:

$$\ddot{\bar{u}} + \dot{\bar{U}_1}\sqrt{\Psi_1}\sqrt{\beta_1} + \dot{\bar{U}_2}\sqrt{\Psi_2}\sqrt{\beta_2} + 2\bar{U}_1\sqrt{\Psi_1}\sqrt{\beta_1}\dot{\bar{u}}' + 2\bar{U}_2\sqrt{\Psi_2}\sqrt{\beta_2}\dot{\bar{u}}' + \Psi_1\bar{U_1}^2\bar{u}'' + \Psi_2\bar{U_2}^2\bar{u}'' + \dot{\bar{U_1}}\sqrt{\Psi_1}\sqrt{\beta_1}\bar{u}' + \dot{\bar{U_2}}\sqrt{\Psi_2}\sqrt{\beta_2}\bar{u}' - \Pi_1\bar{u}'' - (\bar{v}''''\bar{v}' + \bar{v}''\bar{v}''') + (\Pi_0 - \Pi_2 - \Pi_1(\alpha\Delta T) - \Pi_1)\bar{v}'\bar{v}'' - \left(\Pi_0 - \Pi_2 - \Pi_1(\alpha\Delta T)\right)' + \gamma = 0, \quad (23)$$

$$\ddot{\bar{v}} + 2\bar{U}_1\sqrt{\Psi_1}\sqrt{\beta_1}\dot{\bar{v}}' + 2\bar{U}_2\sqrt{\Psi_2}\sqrt{\beta_2}\dot{\bar{v}}' + \Psi_1\bar{U_1}^2\bar{v}'' + \Psi_2\bar{U_2}^2\bar{v}'' - a\Psi_1\bar{U_1}^2\bar{v}'' - a\Psi_2\bar{U_2}^2\bar{v}'' + \dot{\bar{U_1}}\sqrt{\Psi_1}\sqrt{\beta_1}\bar{v}' + \dot{\bar{U_2}}\sqrt{\Psi_2}\sqrt{\beta_2}\bar{v}' - \left(\Pi_0 - \Pi_2 - \Pi_1(\alpha\Delta T)\right)v'' + \bar{v}'''' - \left(3\bar{u}'''\bar{v}'' + 4\bar{v}'''\bar{u}'' + 2\bar{u}'\bar{v}'''' + 2\bar{v}'^2\bar{v}'''' + 8\bar{v}'\bar{v}''\bar{v}''' + 2\bar{v}''^3\right) + (\Pi_0 - \Pi_2 - \Pi_1(\alpha\Delta T) - \Pi_1)\left(\bar{u}'\bar{v}'' + \bar{v}'\bar{u}'' + \frac{3}{2}\bar{v}'^2\bar{v}''\right) = 0 \quad (24)$$

The associated dimensionless boundary conditions are:

$$\bar{v}(0) = \bar{v}'(0) \; and \; \bar{v}''(L) = \bar{v}'''(L) = 0 \quad (25)$$

$$\bar{u}(0) = \bar{u}'(L) = 0 \quad (26)$$

Preprints (www.preprints.org) | NOT PEER-REVIEWED | Posted: 6 October 2017 doi:10.20944/preprints201710.0030.v1

Peer-reviewed version available at Math. Comput. Appl. 2017, 22, 44; doi:10.3390/mca22040044

1.2.3 Governing Equation for a steady two-phase flow

$$\ddot{\bar{u}} + \bar{U}_1 C21\dot{\bar{u}}' + \bar{U}_2 C22\dot{\bar{u}}' + C31\overline{U_1}^2\bar{u}'' + C32\overline{U_2}^2\bar{u}'' - C5\bar{u}'' - (\bar{v}''''\bar{v}' + \bar{v}''\bar{v}''') + C6\bar{v}'\bar{v}'' - C7' + \gamma = 0 \quad (27)$$

$$\ddot{\bar{v}} + \bar{U}_1 C21\dot{\bar{v}}' + \bar{U}_2 C22\dot{\bar{v}}' + C31\overline{U_1}^2\bar{v}'' + C32\overline{U_2}^2\bar{v}'' - aC31\overline{U_1}^2\bar{v}'' - aC32\overline{U_2}^2\bar{v}'' - C7v'' + \bar{v}'''' - \left(3\bar{u}'''\bar{v}'' + 4\bar{v}'''\bar{u}'' + 2\bar{u}'\bar{v}'''' + 2\bar{v}'^2\bar{v}'''' + 8\bar{v}'\bar{v}''\bar{v}''' + 2\bar{v}''^3\right) + C6\left(\bar{u}'\bar{v}'' + \bar{v}'\bar{u}'' + \frac{3}{2}\bar{v}'^2\bar{v}''\right) = 0 \quad (28)$$

For a steady flow, velocities are not changing with time, therefore $\dot{\overline{U_1}} = \dot{\overline{U_2}} = 0$ (29)

The associated boundary conditions are:

$$\bar{v}(0) = \bar{v}'(0) \; and \; \bar{v}''(L) = \bar{v}'''(L) = 0 \quad (30)$$

$$\bar{u}(0) = \bar{u}'(L) = 0 \quad (31)$$

Equations (27) to (31) are obtained using the notations:

$$C11 = \sqrt{\Psi_1}\sqrt{\beta_1}\,,\; C12 = \sqrt{\Psi_2}\sqrt{\beta_2}\,,\; C21 = 2\sqrt{\Psi_1}\sqrt{\beta_1}\,,\; C22 = 2\sqrt{\Psi_2}\sqrt{\beta_2}\,,\; C31 = \Psi_1$$

$$C32 = \Psi_2,\; C5 = \Pi_1,\; C6 = (\Pi_0 - \Pi_2 - \Pi_1(\alpha\Delta T) - \Pi_1),\; C7 = \Pi_0 - \Pi_2 - \Pi_1(\alpha\Delta T)$$

1.3 Empirical gas–liquid two-phase flow model

The components velocities in terms of the superficial velocities are expressed as:

$$V_g = U_g vf, \quad V_l = U_l(1 - vf) \quad (32)$$

Where U_g and U_l are the superficial flow velocities.

Adopting the Chisholm empirical relations as presented in [24],

Void fraction:

$$vf = \left[1 + \sqrt{1 - \mathrm{x}\left(1 - \frac{\rho_l}{\rho_g}\right)}\left(\frac{1-\mathrm{x}}{\mathrm{x}}\right)\left(\frac{\rho_g}{\rho_l}\right)\right]^{-1} = \frac{\text{Volume of gas}}{\text{Volume of gas+Volume of Liquid}} \quad (33)$$

Slip Ratio:

$$S = \frac{V_g}{V_l} = \left[1 - \mathrm{x}\left(1 - \frac{\rho_l}{\rho_g}\right)\right]^{1/2} \quad (34)$$

The vapour quality: (x)

The densities of the liquid and gas phases respectively: (ρ_l and ρ_g)

Preprints (www.preprints.org) | NOT PEER-REVIEWED | Posted: 6 October 2017 doi:10.20944/preprints201710.0030.v1

Peer-reviewed version available at Math. Comput. Appl. 2017, 22, 44; doi:10.3390/mca22040044

Mixture Velocity:

$$V_T = U_g vf + U_l(1 - vf) \tag{35}$$

Individual Velocities:

$$V_l = \frac{V_T}{S+1}, V_g = \frac{SV_T}{S+1} \tag{36}$$

For various void fractions (0.3, 0.4, and 0.5) and a series of mixture velocities, the corresponding slip ratio and individual velocities are estimated and used for numerical calculations.

2 Method of Solution

Exact solutions of nonlinear equations are almost not available; an approximate solution will be sought for by utilizing the multiple time scale perturbation technique. This approach is applied directly to the partial differential equations (27) and (28), given that the common method of discretizing the equations first and then applying perturbation method yields less accurate results for finite mode truncations and higher order perturbation schemes [14, 15, 16 and 17].

Adopting perturbation techniques, it is necessary to decide the terms to be considered small or weak. However, the study considers the contributions of the nonlinear terms, gradient term and gravity term to be small compared to the linear terms.

$$\ddot{\bar{u}} + \bar{U}_1 C21\dot{\bar{u}}' + \bar{U}_2 C22\dot{\bar{u}}' + C31\overline{U_1}^2\bar{u}'' + C32\overline{U_2}^2\bar{u}'' - C5\bar{u}'' + \varepsilon\left(-(\bar{v}''''\bar{v}' + \bar{v}''\bar{v}''') + C6\bar{v}'\bar{v}'' - C7' + \gamma_j\right) = 0, \tag{37}$$

$$\ddot{\bar{v}} + \bar{U}_1 C21\dot{\bar{v}}' + \bar{U}_2 C22\dot{\bar{v}}' + C31\overline{U_1}^2\bar{v}'' + C32\overline{U_2}^2\bar{v}'' - aC31\overline{U_1}^2\bar{v}'' - aC32\overline{U_2}^2\bar{v}'' - C7v'' + \bar{v}'''' + \varepsilon\left(-\left(3\bar{u}'''\bar{v}'' + 4\bar{v}'''\bar{u}'' + 2\bar{u}'\bar{v}'''' + 2\bar{v}'^2\bar{v}'''' + 8\bar{v}'\bar{v}''\bar{v}''' + 2\bar{v}''^3\right) + C6\left(\bar{u}'\bar{v}'' + \bar{v}'\bar{u}'' + \frac{3}{2}\bar{v}'^2\bar{v}''\right)\right) = 0 \tag{38}$$

We seek an approximate solution for $\bar{u}$ *and* $\bar{v}$ in the form:

$$\bar{u} = \bar{u}_0(T_0, T_1) + \varepsilon\bar{u}_1(T_0, T_1) + \varepsilon^2\bar{u}_2(T_0, T_1) + O(\varepsilon) \tag{39}$$

$$\bar{v} = \bar{v}_0(T_0, T_1) + \varepsilon\bar{v}_1(T_0, T_1) + \varepsilon^2\bar{v}_2(T_0, T_1) + O(\varepsilon) \tag{40}$$

Two time scales are needed $T_0 = t$ and $T_1 = \varepsilon t$

Where ε is a small dimensionless measure of the amplitude of $\bar{u}$ and $\bar{v}$, used as a book-keeping parameter. Then, the time derivatives are:

$$\frac{d}{dt} = D_0 + \varepsilon D_1 + \varepsilon^2 D_2 + O(\varepsilon) \tag{41}$$

$$\frac{d^2}{dt^2} = {D_0}^2 + 2\varepsilon D_0 D_1 + \varepsilon^2({D_1}^2 + 2D_0 D_2) + O(\varepsilon) \tag{42}$$

$$Where\ D_n = \frac{\partial}{\partial T_n}$$

Preprints (www.preprints.org) | NOT PEER-REVIEWED | Posted: 6 October 2017 doi:10.20944/preprints201710.0030.v1

Peer-reviewed version available at Math. Comput. Appl. 2017, 22, 44; doi:10.3390/mca22040044

Substituting Eq. (42), Eq. (41), Eq. (40) and Eq. (39) into Eq. (37) and Eq. (38) and equating the coefficients of (ε) to zero and one respectively:

U-Equation:

$$O(\varepsilon^0). \quad {D_0}^2\bar{u}_0 + C21D_0\bar{u}_0'\bar{U}_1 + C22D_0\bar{u}_0''\bar{U}_2 + C31\bar{u}_0''{\bar{U}_1}^2 + C32\bar{u}_0''{\bar{U}_2}^2 - C5\bar{u}_0'' = 0 \qquad (43)$$

$$O(\varepsilon^1). \quad {D_0}^2\bar{u}_1 + C21D_0\bar{u}_1'\bar{U}_1 + C22D_0\bar{u}_1'\bar{U}_2 + 2D_1D_0\bar{u}_0 + C31\bar{u}_1''{\bar{U}_1}^2 + C32\bar{u}_1''{\bar{U}_2}^2 + C21D_0\bar{u}_0'\bar{U}_1 + C22D_0\bar{u}_0'\bar{U}_2 - C5\bar{u}_1'' - \bar{v}_0''''\bar{v}_0' - C7' + \gamma - \bar{v}_0''\bar{v}_0''' + C6\bar{v}_0'\bar{v}_0'' = 0 \qquad (44)$$

V-Equation:

$$O(\varepsilon^0). \quad {D_0}^2\bar{v}_0 - C7\bar{v}_0'' + \bar{v}_0'''' + C21D_0\bar{v}_0'\bar{U}_1 + C22D_0\bar{v}_0'\bar{U}_2 + C31\bar{v}_0''{\bar{U}_1}^2 + C32\bar{v}_0''{\bar{U}_2}^2 - aC31\bar{v}_0''{\bar{U}_1}^2 - aC32\bar{v}_0''{\bar{U}_2}^2 = 0 \qquad (45)$$

$$O(\varepsilon^1). \quad {D_0}^2\bar{v}_1 - C7\bar{v}_1'' + \bar{v}_1'''' - 2\bar{u}_0'\bar{v}_0'''' - 4\bar{u}_0''\bar{v}_0''' - 3\bar{v}_0''\bar{v}_0''' - 2{\bar{v}_0}^{3''} + 2D_0D_1\bar{v}_0 + C31\bar{v}_1''{\bar{U}_1}^2 + C32\bar{v}_1''{\bar{U}_2}^2 - 8\bar{v}_0'\bar{v}_0''\bar{v}_0''' + C6\bar{u}_0'\bar{v}_0'' + C6\bar{u}_0''\bar{v}_0' + \frac{3}{2}C6{\bar{v}_0}^{2'}\bar{v}_0'' + C21D_0\bar{v}_0'\bar{U}_1 + C22D_0\bar{v}_0'\bar{U}_2 + C21D_1\bar{v}_0'\bar{U}_1 + C22D_1\bar{v}_0'\bar{U}_2 - aC31\bar{v}_1''{\bar{U}_1}^2 - aC32\bar{v}_1''{\bar{U}_2}^2 = 0 \qquad (46)$$

The order zero problems for both the axial and transverse vibration of the cantilever pipe have the form of an undamped and unforced flow induced vibration problem. This will be used to estimate the linear natural frequencies and mode shapes while the order problem will be solved to obtain the amplitude of the nonlinear response of the pipe.

2.1 Linear Analysis

The leading order equations present a set of linear equations which relates the flow velocity generated forces (Coriolis and Centrifugal forces) to the stiffness of the pipe and not neglecting the mass ratios. These set of linear equations exhibits the form of an eigenvalue problem, which upon resolution will produce the natural frequency, mode shapes and also predict the stability of the system,

2.1.1 Natural frequencies and modal functions

Estimation of the Natural frequencies and modal function is an order zero problem that can be determined by resolving Eq. (43) and Eq. (45).

The homogeneous solution of the leading order equations Eq. (43) and Eq. (45) can be expressed as:

$$\bar{u}(x, T_0, T_1)_0 = \phi(x)_n \, exp(i\omega_n T_0) + CC \qquad (47)$$

$$\bar{v}(x, T_0, T_1)_0 = \eta(x)_n \, exp(i\lambda_n T_0) + CC \qquad (48)$$

Where (CC) is the complex conjugate, $\phi(x)_n \; and \; \eta(x)_n$ are the complex modal functions for the axial and transverse vibrations for each mode (n) and $\omega_n \; and \; \lambda_n$ are the eigenvalues for the axial and transverse vibrations for each mode (n).The eigenvalues are complex values with complex conjugate pair of solutions which can be expressed as:

$$\omega_n = Re(\omega_n) + iIm(\omega_n) \; and \; \overline{\omega_n} = Re(\omega_n) - iIm(\omega_n)$$

$$\lambda_n = Re(\omega_n) + iIm(\lambda_n) \; and \; \overline{\lambda_n} = Re(\lambda_n) - iIm(\lambda_n)$$

Preprints (www.preprints.org) | NOT PEER-REVIEWED | Posted: 6 October 2017 doi:10.20944/preprints201710.0030.v1

Peer-reviewed version available at Math. Comput. Appl. 2017, 22, 44; doi:10.3390/mca22040044

The real parts of the eigenvalues are associated with the natural frequency of oscillation and the imaginary part with the damping.

Substituting Eq. (47) and Eq. (48) into Eq. (43) and Eq. (45) respectively, results to:

$$\left(C31\bar{U}_1{}^2 + C32\bar{U}_2{}^2 - C5\right)\phi(x)_n{}'' + (C21\bar{U}_1 + C22\bar{U}_2)i\omega_n\phi(x)_n{}' - \phi(x)_n\omega_n{}^2 = 0 \quad (49)$$

$$\eta(x)_n{}'''' + \left(C31\bar{U}_1{}^2 + C32\bar{U}_2{}^2 - C7 - aC31\bar{U}_1{}^2 - aC32\bar{U}_2{}^2\right)\eta(x)_n{}'' + (C21\bar{U}_1 + C22\bar{U}_2)i\lambda_n\eta(x)_n{}' - \eta(x)_n\lambda_n{}^2 = 0 \quad (50)$$

The general solution to the ordinary differential equations Eq. (49) and Eq. (50) are expressed as:

$$\phi(x)_n = G1_n\, exp(ik_1x) + G2_n\, exp(ik_2x) \quad (51)$$

$$\eta(x)_n = H1(exp(iz_1x) + H2exp(iz_2x) + H3\, exp(iz_3x) + H4ex\, p(iz_4x) \quad (52)$$

2.1.2 Solution to axial vibration problem

Substituting Eq. (51) into Eq. (49) gives a quadratic relation of the form:

$$\left(C5 - C31\bar{U}_1{}^2 - C32\bar{U}_2{}^2\right)k_j{}^2 - (C21\bar{U}_1 + C22\bar{U}_2)i\omega_nk_j - \omega_n{}^2 = 0 \quad (53)$$

Solving the quadratic equation (53) for the wave numbers (k_j) as a function of the eigenvalue (ω_n):

$$k_1 = \omega_n\left[\frac{\frac{C21\bar{U}_1}{2} + \frac{C22\bar{U}_2}{2} + \frac{\sqrt{C21^2\bar{U}_1{}^2 + 2C21C22\bar{U}_1\bar{U}_2 + C22^2\bar{U}_2{}^2 - 4C31\bar{U}_1{}^2 - 4C32\bar{U}_2{}^2 + 4C5}}{2}}{C5 - C31\bar{U}_1{}^2 - C32\bar{U}_2{}^2}\right] \quad (54)$$

$$k_2 = \omega_n\left[\frac{\frac{C21\bar{U}_1}{2} + \frac{C22\bar{U}_2}{2} - \frac{\sqrt{C21^2\bar{U}_1{}^2 + 2C21C22\bar{U}_1\bar{U}_2 + C22^2\bar{U}_2{}^2 - 4C31\bar{U}_1{}^2 - 4C32\bar{U}_2{}^2 + 4C5}}{2}}{C5 - C31\bar{U}_1{}^2 - C32\bar{U}_2{}^2}\right] \quad (55)$$

In order to obtain the eigenvalue, Eq. (51) is substituted into the boundary conditions in Eq. (31):

$$\frac{\partial\phi(l,t)}{\partial x} = 0\ and\ \phi(0,t) = 0 \quad (56)$$

$$G1 + G2 = 0 \quad (57)$$

$$and$$

$$G1k1i\, exp(iLk_1) + G2k2i\, exp(iLk_2) = 0 \quad (58)$$

Preprints (www.preprints.org) | NOT PEER-REVIEWED | Posted: 6 October 2017 doi:10.20944/preprints201710.0030.v1

Peer-reviewed version available at Math. Comput. Appl. 2017, 22, 44; doi:10.3390/mca22040044

In matrix form:

$$\underbrace{\begin{pmatrix} 1 & 1 \\ ik_1 exp(iLk_1) & ik_2 exp(iLk_2) \end{pmatrix}}_{D} \begin{pmatrix} G1 \\ G2 \end{pmatrix} = 0 \qquad (59)$$

For a non-trivial solution, the determinant of (D) must varnish;

$$-ik_1\, exp(iLk_1) + ik_2\, exp(iLk_2) = 0 \qquad (60)$$

Substituting Eq. (54) and Eq. (55) into Eq. (60) and solving for the eigenvalue:

$$\omega_n = \frac{2\pi n - i.ln\left(\frac{b}{a}\right)}{(a-b)L}, \qquad n = 1,2,3,\ldots \qquad (61)$$

Where:

$$a = \frac{\frac{C21\bar{U}_1}{2} + \frac{C22\bar{U}_2}{2} + \frac{\sqrt{C21^2\bar{U}_1{}^2 + 2C21C22\bar{U}_1\bar{U}_2 + C22^2\bar{U}_2{}^2 - 4C31\bar{U}_1{}^2 - 4C32\bar{U}_2{}^2 + 4C5}}{2}}{C5 - C31\bar{U}_1{}^2 - C32\bar{U}_2{}^2},$$

$$b = \frac{\frac{C21\bar{U}_1}{2} + \frac{C22\bar{U}_2}{2} - \frac{\sqrt{C21^2\bar{U}_1{}^2 + 2C21C22\bar{U}_1\bar{U}_2 + C22^2\bar{U}_2{}^2 - 4C31\bar{U}_1{}^2 - 4C32\bar{U}_2{}^2 + 4C5}}{2}}{C5 - C31\bar{U}_1{}^2 - C32\bar{U}_2{}^2}$$

Eq. (61) is the pipe's axial vibration eigenvalue. Solving Eq. (57) and Eq. (58) gives the constants G1 and G2. Therefore, the modal function for the axial vibration of the pipe is expressed as:

$$\phi(x)_n = G1_n\, exp(ik_1 x) + G2_n\, exp(ik_2 x) \qquad (62)$$

Substituting Eq. (51) into Eq. (47) yields:

$$\bar{u}(x,T_0)_0 = \sum_{j=1}^{2} G_{jn}\, exp\left(ik_{jn}x\right) exp(i\omega_n T_0) = \sum_{j=1}^{2} G_{jn}\, exp\left(-Im\left(k_{jn}x\right) - Im(\omega_n T_0)\right) exp\left(i(Re\left(k_{jn}x\right) + Re(\omega_n T_0))\right) \qquad (63)$$

It can be observed from Eq. (63) that the real part is the natural frequency and the imaginary part is the amplitude. However as the mixture velocity is varied, a critical value of the mixture velocity is attained when the imaginary parts of any of the eigenvalues (ω_n) will have a negative value which will cause the axial displacement ($\bar{u}$) to grow exponentially in time and this linearly signifies the onset of the system's oscillatory instability.

Preprints (www.preprints.org) | NOT PEER-REVIEWED | Posted: 6 October 2017 doi:10.20944/preprints201710.0030.v1

Peer-reviewed version available at Math. Comput. Appl. 2017, 22, 44; doi:10.3390/mca22040044

2.1.3 Solution to transverse vibration problem

Substituting Eq. (52) into Eq. (50) gives a quartic relation:

$$z^4{}_{jn} + \left(C7 - C31\bar{U}_1{}^2 - C32\bar{U}_2{}^2 + aC31\bar{U}_1{}^2 + aC32\bar{U}_2{}^2\right) z^2{}_{jn} - (C21\bar{U}_1 + C22\bar{U}_2) z_{jn}\lambda_n - \lambda^2{}_n = 0 \quad (64)$$

$j = 1,2,3,4\ and\ n = 1,2,3,4,5\ldots$

In order to obtain the eigenvalue, Eq. (52) is substituted into the boundary conditions in Eq. (30):

This gives four algebraic equations which can be expressed in matrix form as:

$$\underbrace{\begin{bmatrix} 1 & 1 & 1 & 1 \\ z_{1n} & z_{2n} & z_{3n} & z_{4n} \\ (z_{1n})^2.\exp(i.z_{1n}) & (z_{2n})^2.\exp(i.z_{2n}) & (z_{3n})^2.\exp(i.z_{3n}) & (z_{4n})^2.\exp(i.z_{4n}) \\ (z_{1n})^3.\exp(i.z_{1n}) & (z_{2n})^3.\exp(i.z_{2n}) & (z_{3n})^3.\exp(i.z_{3n}) & (z_{4n})^3.\exp(i.z_{4n}) \end{bmatrix}}_{G} \cdot \begin{bmatrix} 1 \\ H2_n \\ H3_n \\ H4_n \end{bmatrix} . H1_n = \begin{pmatrix} 0 \\ 0 \\ 0 \\ 0 \end{pmatrix} \quad (65)$$

For a non-trivial solution, the determinant of (G) must varnish, That is:

$$DET(G) = 0 \quad (66)$$

In order to find modal solutions of (λ_n), Eq. (64) and Eq. (65) must be solved simultaneously, this can be solved numerically using nonlinear numerical routine.

The mode function of the transverse vibration corresponding to the nth eigenvalue is expressed as:

$$\eta(x)_n = H1_n.[e^{x.z_{1n}.i} - (A + B + C + D) - E] \quad (67)$$

$$A = \frac{e^{x.z_{4n}.i}.\ [e^{z_{1n}.i}.(z_{1n})^3.z_{2n} - e^{z_{1n}.i}.(z_{1n})^3.\ z_{3n} - e^{z_{1n}.i}.\ z_{4n}.(z_{1n})^2.z_{2n}}{(z_{2n} - z_{4n}).(z_{3n} - z_{4n}).[e^{z_{2n}.i}.(z_{2n})^2 - e^{z_{3n}.i}.(z_{3n})^2]}$$

$$B = \frac{e^{x.z_{4n}.i}.\ [e^{z_{1n}.i}.z_{4n}.(z_{1n})^2.z_{3n} - e^{z_{2n}.i}.z_{1n}.(z_{2n})^3 + e^{z_{2n}.i}.\ z_{4n}.z_{1n}.(z_{2n})^2}{(z_{2n} - z_{4n}).(z_{3n} - z_{4n}).[e^{z_{2n}.i}.(z_{2n})^2 - e^{z_{3n}.i}.(z_{3n})^2]}$$

$$C = \frac{e^{x.z_{4n}.i}.\ [e^{z_3.i}.z_{1n}.(z_{3n})^3 - e^{z_3.i}.z_{4n}.z_{1n}.(z_{3n})^2 + e^{z_{2n}.i}.(z_{2n})^3.z_{3n}}{(z_{2n} - z_{4n}).(z_{3n} - z_{4n}).[e^{z_{2n}.i}.(z_{2n})^2 - e^{z_{3n}.i}.(z_{3n})^2]}$$

$$D = \frac{e^{x.z_{4n}.i}.\ [-e^{z_{2n}.i}.z_{4n}.(z_{2n})^2.z_{3n} - e^{z_3.i}.z_{2n}.(z_{3n})^3 + e^{z_3.i}.z_{4n}.z_{2n}.(z_{3n})^2}{(z_{2n} - z_{4n}).(z_{3n} - z_{4n}).[e^{z_{2n}.i}.(z_{2n})^2 - e^{z_{3n}.i}.(z_{3n})^2]}$$

$$E = \frac{e^{x.z_{2n}.i}.(z_{1n} - z_{4n}).[e^{z_1.i}.\ (z_{1n})^2 - e^{z_3.i}.(z_{3n})^2]}{(z_{2n} - z_{4n}).\ [e^{z_2.i}.(z_{2n})^2 - e^{z_3.i}.(z_{3n})^2]} + \frac{e^{x.z_3.i}.(z_{1n} - z_{4n}).[e^{z_{1n}.i}.\ (z_{1n})^2 - e^{z_2 i}.(z_{2n})^2]}{(z_{3n} - z_{4n}).\ [e^{z_2.i}.(z_{2n})^2 - e^{z_3.i}.(z_{3n})^2]}$$

Substituting Eq. (52) into Eq. (48) yields:

$$\bar{v}(x, T_0)_0 = \sum_{j=1}^{4} H_{jn}\, exp(iz_{jn}x)\, exp(i\lambda_n T_0) = \sum_{j=1}^{4} H_{jn}\, exp\left(-Im(z_{jn}x) - Im(\lambda_n T_0)\right) exp\left(i(Re(z_{jn}x) + Re(\lambda_n T_0))\right) \quad (68)$$

It can be observed from Eq. (68) that the real part is the natural frequency and the imaginary part is the amplitude. However as the mixture velocity is varied, a critical value of the mixture velocity is attained when the imaginary parts of any of the eigenvalues (λ_n) will have a negative value which will cause the transverse displacement $(\bar{v})$ to grow exponentially in time and this linearly signifies the onset of the system's flutter instability.

Preprints (www.preprints.org) | NOT PEER-REVIEWED | Posted: 6 October 2017 doi:10.20944/preprints201710.0030.v1

Peer-reviewed version available at Math. Comput. Appl. 2017, 22, 44; doi:10.3390/mca22040044

2.2 Nonlinear Analysis

Linear analysis of the system is sufficient for the prediction of the critical velocity at which instability will occur but cannot predict the post buckling behaviour. Linear theory has shown that buckling amplitudes will grow unboundedly with time after the critical velocity, however, as amplitudes grow, effect of nonlinearities comes into play. This predictably limits the growth to some finite value [21-23].

2.2.1 Nonlinear axial and transverse vibration problem

The solution to the nonlinear axial and transverse vibration problem by seeking an approximate solution for $\bar{u}\ and\ \bar{v}$ of the form:

$$\bar{u} = \bar{u}_0(T_0, T_1) + \varepsilon\bar{u}_1(T_0, T_1) + \varepsilon^2\bar{u}_2(T_0, T_1) + O(\varepsilon) \quad (69)$$
$$\bar{v} = \bar{v}_0(T_0, T_1) + \varepsilon\bar{v}_1(T_0, T_1) + \varepsilon^2\bar{v}_2(T_0, T_1) + O(\varepsilon) \quad (70)$$

The zero order solutions produced the undamped and uncoupled linear solution of the axial and transverse vibration respectively as:

$$\bar{u}(x, T_0, T_1)_0 = \phi(x)\, X(T_1) exp(i\omega T_0) + CC \quad (71)$$
$$\bar{v}(x, T_0, T_1)_0 = \eta(x) Y(T_1)\, exp(i\lambda T_0) + CC \quad (72)$$

Where X and Y are unknown complex-valued functions of the slow time scale T_1, (CC) is the complex conjugate, $\phi(x)\ and\ \eta(x)$ are the modal functions for the axial and transverse vibrations for and $\omega = Re(\omega) and\ \lambda = Re(\lambda)$ (The real parts of the complex frequencies) are the natural frequencies for the axial and transverse vibrations.

Substituting Eq. (71) and Eq. (72) into the equations (44) and (46) gives;

$$D_0{}^2\bar{u}_1 - C5\bar{u}_1'' + C21D_0\bar{u}_1'\bar{U}_1 + C22D_0\bar{u}_1'\bar{U}_2 + C31\bar{u}_1''\bar{U}_1{}^2 + C32\bar{u}_1''\bar{U}_2{}^2 = -\left(C21\frac{\partial X(T1)}{\partial T1}\frac{\partial\phi(x)}{\partial x}\bar{U}_1 + C22\frac{\partial X(T1)}{\partial T1}\frac{\partial\phi(x)}{\partial x}\bar{U}_2 + 2i\frac{\partial X(T1)}{\partial T1}\omega\right) exp(i\omega T_0) + Y(T1)^2\left(\frac{\partial\eta(x)}{\partial x}\frac{\partial^4\eta(x)}{\partial x^4} + \frac{\partial^2\eta(x)}{\partial x^2}\frac{\partial^3\eta(x)}{\partial x^3} - C6\frac{\partial\eta(x)}{\partial x}\frac{\partial^2\eta(x)}{\partial x^2}\right) exp(2i\lambda T_0) + NST + CC = 0 \quad (73)$$

$$D_0{}^2\bar{v}_1 - C7\bar{v}_1'' + \bar{v}_1'''' + C21D_0\bar{v}_1'\bar{U}_1 + C22D_0\bar{v}_1'\bar{U}_2 + C31\bar{v}_1''\bar{U}_1{}^2 + C32\bar{v}_1''\bar{U}_2{}^2 - aC31\bar{v}_1''\bar{U}_1{}^2 - aC32\bar{v}_1''\bar{U}_2{}^2 = \left(\frac{\partial Y(T1)}{\partial T1}\left(C21\frac{\partial\eta(x)}{\partial x}\bar{U}_1 + C22\frac{\partial\eta(x)}{\partial x}\bar{U}_2 + 2\eta(x)\lambda i\right) + 6Y(T1)^2\overline{Y(T1)}\left(\frac{\partial\eta(x)}{\partial x}\right)^2\frac{\partial\overline{\eta(x)}}{\partial x} + 2Y(T1)^2\overline{Y(T1)}\left(\frac{\partial\eta(x)}{\partial x}\right)^2\frac{\partial^4\overline{\eta(x)}}{\partial x^4} + 4Y(T1)^2\overline{Y(T1)}\frac{\partial\eta(x)}{\partial x}\frac{\partial\overline{\eta(x)}}{\partial x}\frac{\partial^4\eta(x)}{\partial x^4} + 8Y(T1)^2\overline{Y(T1)}\frac{\partial\eta(x)}{\partial x}\frac{\partial^2\overline{\eta(x)}}{\partial x^2}\frac{\partial^3\eta(x)}{\partial x^3} + 8Y(T1)^2\overline{Y(T1)}\frac{\partial\overline{\eta(x)}}{\partial x}\frac{\partial^2\eta(x)}{\partial x^2}\frac{\partial^3\eta(x)}{\partial x^3} - 3C6.Y(T1)^2\overline{Y(T1)}\frac{\partial\eta(x)}{\partial x}\frac{\partial\overline{\eta(x)}}{\partial x}\frac{\partial^2\eta(x)}{\partial x^2} + 8Y(T1)^2\overline{Y(T1)}\frac{\partial\eta(x)}{\partial x}\frac{\partial^2\eta(x)}{\partial x^2}\frac{\partial^3\overline{\eta(x)}}{\partial x^3} - \frac{3}{2}C6.Y(T1)^2\overline{Y(T1)}\left(\frac{\partial\eta(x)}{\partial x}\right)^2\frac{\partial^2\eta(x)}{\partial x^2}\right) exp(i\lambda T_0) + \left(2X(T1)\overline{Y(T1)}\frac{\partial\Phi(x)}{\partial x}\frac{\partial^4\overline{\eta(x)}}{\partial x^4} + 4X(T1)\overline{Y(T1)}\frac{\partial^2\Phi(x)}{\partial x^2}\frac{\partial^3\overline{\eta(x)}}{\partial 3}\right) exp(i\omega T_0)\, exp(-i\lambda T_0) - \left(C6X(T1)\overline{Y(T1)}\frac{\partial\Phi(x)}{\partial x}\frac{\partial^2\overline{\eta(x)}}{\partial x^2} + C6X(T1)\overline{Y(T1)}\frac{\partial\overline{\eta(x)}}{\partial x}\frac{\partial^2\Phi(x)}{\partial x^2}\right) exp(i\omega T_0)\, exp(-i\lambda T_0) + 3Y(T1)^2\frac{\partial^2\eta(x)}{\partial x^2}\frac{\partial^3\eta(x)}{\partial x^3} exp(2i\lambda T_0) + NST + CC = 0 \quad (74)$$

Where CC and NST denote complex conjugates and non-secular terms respectively

Preprints (www.preprints.org) | NOT PEER-REVIEWED | Posted: 6 October 2017 doi:10.20944/preprints201710.0030.v1

Peer-reviewed version available at Math. Comput. Appl. 2017, 22, 44; doi:10.3390/mca22040044

The next task is to determine the requirements for X(T1) and Y(T1) that permits the solutions of $\bar{u}_1$ and $\bar{v}_1$ to be independent of secular terms. However, examining equations (73) and (74), it can be observed that two scenarios exist $\omega \neq 2\lambda$ and $\omega = 2\lambda$.

2.2.2 When ω is far from 2λ

If ω is far from 2λ, then none of the coupled nonlinear terms will generate secular terms, therefore resulting to uncoupled response.

The two equations (73) and (74) will have bounded solutions only if solvability condition holds. The solvability condition demands that the coefficient of $exp(i\omega T_0)$ and $exp(i\lambda T_0)$. That is, X (T1) and Y (T1) should satisfy the following relation:

$$-\left(\mathrm{C21}\frac{\partial \mathrm{X(T1)}}{\partial \mathrm{T1}}\frac{\partial \phi(x)}{\partial \mathrm{x}}\bar{U}_1 + \mathrm{C22}\frac{\partial \mathrm{X(T1)}}{\partial \mathrm{T1}}\frac{\partial \phi(x)}{\partial \mathrm{x}}\bar{U}_2 + 2\mathrm{i}\frac{\partial \mathrm{X(T1)}}{\partial \mathrm{T1}}\phi(x)\omega\right) = 0 \quad (75)$$

$$\left(\frac{\partial Y(T1)}{\partial T1}\left(C21\frac{\partial \eta(x)}{\partial x}\bar{U}_1 + C22\frac{\partial \eta(x)}{\partial x}\bar{U}_2 + 2\eta(x)\lambda i\right) + 6Y(T1)^2\overline{Y(T1)}\left(\frac{\partial \eta(x)}{\partial x}\right)^2\frac{\partial \overline{\eta(x)}}{\partial x} + 2Y(T1)^2\overline{Y(T1)}\left(\frac{\partial \eta(x)}{\partial x}\right)^2\frac{\partial^4\overline{\eta(x)}}{\partial x^4} + 4Y(T1)^2\overline{Y(T1)}\frac{\partial \eta(x)}{\partial x}\frac{\partial \overline{\eta(x)}}{\partial x}\frac{\partial^4\eta(x)}{\partial x^4} + 8Y(T1)^2\overline{Y(T1)}\frac{\partial \eta(x)}{\partial x}\frac{\partial^2\overline{\eta(x)}}{\partial x^2}\frac{\partial^3\eta(x)}{\partial x^3} + 8Y(T1)^2\overline{Y(T1)}\frac{\partial \overline{\eta(x)}}{\partial x}\frac{\partial^2\eta(x)}{\partial x^2}\frac{\partial^3\eta(x)}{\partial x^3} - 3C6.Y(T1)^2\overline{Y(T1)}\frac{\partial \eta(x)}{\partial x}\frac{\partial \overline{\eta(x)}}{\partial x}\frac{\partial^2\eta(x)}{\partial x^2} + 8Y(T1)^2\overline{Y(T1)}\frac{\partial \eta(x)}{\partial x}\frac{\partial^2\eta(x)}{\partial x^2}\frac{\partial^3\overline{\eta(x)}}{\partial x^3} - \frac{3}{2}C6.Y(T1)^2\overline{Y(T1)}\left(\frac{\partial \eta(x)}{\partial x}\right)^2\frac{\partial^2\overline{\eta(x)}}{\partial x^2}\right) = 0 \quad (76)$$

With the inner product defined for complex functions on [0, 1] as:

$$\langle f, g\rangle = \int_0^1 f\bar{g}\,dx \quad (77)$$

Equations (88) and (89) can be cast as:

$$\frac{\partial X(T1)}{\partial T1} = 0 \quad (78)$$

$$\frac{\partial Y(T1)}{\partial T1} + SY(T1)^2\overline{Y(T1)} = 0 \quad (79)$$

Where: $S = \frac{\int_0^1\left[6\left(\frac{\partial \eta(x)}{\partial x}\right)^2\frac{\partial \overline{\eta(x)}}{\partial x}+2\left(\frac{\partial \eta(x)}{\partial x}\right)^2\frac{\partial^4\overline{\eta(x)}}{\partial x^4}+4\frac{\partial \eta(x)}{\partial x}\frac{\partial \overline{\eta(x)}}{\partial x}\frac{\partial^4\eta(x)}{\partial x^4}+8\frac{\partial \eta(x)}{\partial x}\frac{\partial^2\overline{\eta(x)}}{\partial x^2}\frac{\partial^3\eta(x)}{\partial x^3}\right]\overline{\eta(x)}dx}{(C21\bar{U}_1+C22\bar{U}_2)\int_0^1\frac{\partial \eta(x)}{\partial x}\overline{\eta(x)}dx+2i\lambda\int_0^1\eta(x)\overline{\eta(x)}dx} +$

$\frac{\int_0^1\left[8\frac{\partial \overline{\eta(x)}}{\partial x}\frac{\partial^2\eta(x)}{\partial x^2}\frac{\partial^3\eta(x)}{\partial x^3}-3C6\frac{\partial \eta(x)}{\partial x}\frac{\partial \overline{\eta(x)}}{\partial x}\frac{\partial^2\eta(x)}{\partial x^2}+8\frac{\partial \eta(x)}{\partial x}\frac{\partial^2\eta(x)}{\partial x^2}\frac{\partial^3\overline{\eta(x)}}{\partial x^3}-\frac{3}{2}C6\left(\frac{\partial \eta(x)}{\partial x}\right)^2\frac{\partial^2\overline{\eta(x)}}{\partial x^2}\right]\overline{\eta(x)}dx}{(C21\bar{U}_1+C22\bar{U}_2)\int_0^1\frac{\partial \eta(x)}{\partial x}\overline{\eta(x)}dx+2i\lambda\int_0^1\eta(x)\overline{\eta(x)}dx}$

Preprints (www.preprints.org) | NOT PEER-REVIEWED | Posted: 6 October 2017 doi:10.20944/preprints201710.0030.v1

Peer-reviewed version available at Math. Comput. Appl. 2017, 22, 44; doi:10.3390/mca22040044

Solving equation (78) for X(T1), gives a constant amplitude solution up to the 1st order of approximation:

$$X(T1) = \alpha x_0 \tag{80}$$

To determine Y (T1), the solution of equation (79) is expressed in polar form as:

$$Y(T1) = \frac{1}{2}\alpha y(T1)e^{i\beta y(T1)} \text{ and } \overline{Y(T1)} = \frac{1}{2}\alpha y(T1)e^{-i\beta y(T1)} \tag{81}$$

Where S is a complex numbers such that:

$$S = S^R + iS^I$$

Substituting equations (81) into equations (79) and sorting the outcome into real and imaginary parts:

Resolving for $\alpha y \text{ and } \beta y$:

Real Part:

$$\frac{d\alpha y(T1)}{dT1} = -\frac{Re(S)\alpha y(T1)^3}{4} \tag{82}$$

$$\alpha y(T1) = \sqrt{\frac{2}{(\alpha y_0 Re(S) + Re(S)T1)}} \tag{83}$$

Imaginary Part:

$$\alpha y(T1)\frac{d\beta y(T1)}{dT1} = \frac{Im(S)\alpha y(T1)^3}{4} \tag{84}$$

$$\beta y(T1) = -\left[\frac{Im(S)}{2Re(S)}(ln|Re(S)T1 + \alpha y_0 Re(S)|)\right] + \left[\beta y_0 - \frac{Im(S)}{2Re(S)}ln(2)\right] \tag{85}$$

Substituting equations (82) and (81) into equations (69)

$$Y(T1) = \frac{1}{\sqrt{2(Re(S)T1 + K_0)}} exp\left(-i\left(\frac{Im(S)}{2Re(S)}(ln|Re(S)T1 + K_0|)\right) + K_1\right) \tag{86}$$

Where K_0 and K_1 are constants expressed as:

$$K_0 = \alpha y_0 Re(S)$$

$$K_1 = -i\left[\beta y_0 - \frac{Im(S)}{2Re(S)}ln(2)\right]$$

αy_0 and βy_0 are arbitrary constants of integration representing the initial conditions.

Preprints (www.preprints.org) | NOT PEER-REVIEWED | Posted: 6 October 2017 doi:10.20944/preprints201710.0030.v1

Peer-reviewed version available at Math. Comput. Appl. 2017, 22, 44; doi:10.3390/mca22040044

Substituting equations (86) and (80) into equations (71) and (72) respectively, the corresponding nonlinear frequencies can be expressed as:

$$\omega_{nl} = \omega \tag{87}$$

$$\lambda_{nl} = \lambda + \varepsilon \frac{Im(S)}{2Re(S)} (\alpha {y_0}^3 + 4\alpha {y_0}^2 + 6\alpha y_0) \tag{88}$$

Therefore, considering the n-th values of αx(T1), αy(T1), βx(T1) and βy(T1) corresponding to the n-th modal functions and the n-th natural frequencies, the n-th solution of uncoupled problem is expressed as:

$$\bar{u}(x,t)_n = \alpha x(T1)_n \phi(x)_n \cos(\omega_n T0) + O(\varepsilon) \tag{89}$$

$$\bar{v}(x,t)_n = \alpha y(T1)_n \eta(x)_n \cos(\lambda_n T0 + \beta y(T1)_n) + O(\varepsilon) \tag{90}$$

Substituting $T0 = t$, $T1 = \varepsilon t$, the first order approximate solution is expressed as:

$$\bar{u}(x,t) = \sum_{n=1}^{\infty} \alpha x_n |\phi(x)_n| \cos(\omega_n t + \varphi x_n) + O(\varepsilon) \tag{91}$$

$$\bar{v}(x,t) = \sum_{n=1}^{\infty} \alpha y_n |\eta(x)_n| \cos(\lambda_n t + \beta y(T1)_n + \varphi y_n) + O(\varepsilon) \tag{92}$$

Where the phase angles $\varphi x_n \; and \; \varphi y_n$ are given by:

$$\tan(\varphi x_n) = \frac{Im\{\phi(x)_n\}}{Re\{\phi(x)_n\}}, \; \tan(\varphi y_n) = \frac{Im\{\eta(x)_n\}}{Re\{\eta(x)_n\}}$$

2.2.3 When ω is close to 2λ

However in order to examine the coupled nonlinear dynamics of the system, which is the scenario when $\omega = 2\lambda$, a detuning parameter σ is introduced.

$$\omega = 2\lambda + \varepsilon\sigma \tag{93}$$

$$2\lambda T0 = \omega T0 - \sigma T1 \; and \; (\omega - \lambda)T0 = \lambda T0 + \sigma T1 \tag{94}$$

The two equations (73) and (74) will have bounded solutions only if solvability condition holds. The solvability condition demands that the coefficient of $exp(i\omega T_0) \; and \; exp(i\lambda T_0)$ vanishes. That is, X (T1) and Y (T1) should satisfy the following relation:

Preprints (www.preprints.org) | NOT PEER-REVIEWED | Posted: 6 October 2017 doi:10.20944/preprints201710.0030.v1

Peer-reviewed version available at Math. Comput. Appl. 2017, 22, 44; doi:10.3390/mca22040044

$$-\left(C21\frac{\partial X(T1)}{\partial T1}\frac{\partial \phi(x)}{\partial x}\bar{U}_1 + C22\frac{\partial X(T1)}{\partial T1}\frac{\partial \phi(x)}{\partial x}\bar{U}_2 + 2i\frac{\partial X(T1)}{\partial T1}\phi(x)\omega\right) + Y(T1)^2\left(\frac{\partial \eta(x)}{\partial x}\frac{\partial^4 \eta(x)}{\partial x^4} + \frac{\partial^2 \eta(x)}{\partial x^2}\frac{\partial^3 \eta(x)}{\partial x^3} - C6\frac{\partial \eta(x)}{\partial x}\frac{\partial^2 \eta(x)}{\partial x^2}\right)exp(-i\sigma T_1) = 0 \quad (95)$$

$$\left(\frac{\partial Y(T1)}{\partial T1}\left(C21\frac{\partial \eta(x)}{\partial x}\bar{U}_1 + C22\frac{\partial \eta(x)}{\partial x}\bar{U}_2 + 2\eta(x)\lambda i\right) + 6Y(T1)^2\overline{Y(T1)}\left(\frac{\partial \eta(x)}{\partial x}\right)^2\frac{\partial \overline{\eta(x)}}{\partial x} + 2Y(T1)^2\overline{Y(T1)}\left(\frac{\partial \eta(x)}{\partial x}\right)^2\frac{\partial^4 \overline{\eta(x)}}{\partial x^4} + 4Y(T1)^2\overline{Y(T1)}\frac{\partial \eta(x)}{\partial x}\frac{\partial \overline{\eta(x)}}{\partial x}\frac{\partial^4 \eta(x)}{\partial x^4} + 8Y(T1)^2\overline{Y(T1)}\frac{\partial \eta(x)}{\partial x}\frac{\partial^2 \overline{\eta(x)}}{\partial x^2}\frac{\partial^3 \eta(x)}{\partial x^3} + 8Y(T1)^2\overline{Y(T1)}\frac{\partial \overline{\eta(x)}}{\partial x}\frac{\partial^2 \eta(x)}{\partial x^2}\frac{\partial^3 \eta(x)}{\partial x^3} - 3C6.Y(T1)^2\overline{Y(T1)}\frac{\partial \eta(x)}{\partial x}\frac{\partial \overline{\eta(x)}}{\partial x}\frac{\partial^2 \eta(x)}{\partial x^2} + 8Y(T1)^2\overline{Y(T1)}\frac{\partial \eta(x)}{\partial x}\frac{\partial^2 \eta(x)}{\partial x^2}\frac{\partial^3 \overline{\eta(x)}}{\partial x^3} - \frac{3}{2}C6.Y(T1)^2\overline{Y(T1)}\left(\frac{\partial \eta(x)}{\partial x}\right)^2\frac{\partial^2 \overline{\eta(x)}}{\partial x^2}\right) + \left(2X(T1)\overline{Y(T1)}\frac{\partial \Phi(x)}{\partial x}\frac{\partial^4 \overline{\eta(x)}}{\partial x^4} + 4X(T1)\overline{Y(T1)}\frac{\partial^2 \Phi(x)}{\partial x^2}\frac{\partial^3 \overline{\eta(x)}}{\partial 3}\right)exp\left(i(\lambda_n T_0 + \sigma T_1)\right) - \left(C6X(T1)\overline{Y(T1)}\frac{\partial \Phi(x)}{\partial x}\frac{\partial^2 \overline{\eta(x)}}{\partial x^2} + C6X(T1)\overline{Y(T1)}\frac{\partial \overline{\eta(x)}}{\partial x}\frac{\partial^2 \Phi(x)}{\partial x^2}\right)exp\left(i(\lambda_n T_0 + \sigma T_1)\right) + 3Y(T1)^2\frac{\partial^2 \eta(x)}{\partial x^2}\frac{\partial^3 \eta(x)}{\partial x^3}exp\left(i(\omega_n T_0 - \sigma T_1)\right) = 0 \quad (96)$$

The equations can be cast as:

$$-\frac{\partial X(T1)}{\partial T1} + J2\,Y(T1)^2 exp(-i\sigma T_1) = 0 \quad (97)$$

$$\frac{\partial Y(T1)}{\partial T1} + K3\left(Y(T1)^2\overline{Y(T1)}\right) + K4\left(X(T)\overline{Y(T1)}\exp(i\sigma T_1)\right) + K5\left(Y(T1)^2\exp(-i\sigma T_1)\right) = 0 \quad (98)$$

Where:

$$J2 = \frac{\int_0^1\left[\frac{\partial \eta(x)\partial^4 \eta(x)}{\partial x\ \partial x^4} + \frac{\partial^2 \eta(x)\partial^3 \eta(x)}{\partial x^2\ \partial x^3} - C6\frac{\partial \eta(x)\partial^2 \eta(x)}{\partial x\ \partial x^2}\right]\overline{\phi(x)}dx}{\int_0^1\left[(C21\bar{U}_1 + C22\bar{U}_2)\frac{d\phi(x)}{dx} + 2i\omega\,\phi(x)\right]\overline{\phi(x)}dx}$$

$$K3 = \frac{\int_0^1\left[6\left(\frac{\partial \eta(x)}{\partial x}\right)^2\frac{\partial \overline{\eta(x)}}{\partial x} + 2\left(\frac{\partial \eta(x)}{\partial x}\right)^2\frac{\partial^4 \overline{\eta(x)}}{\partial x^4} + 4\frac{\partial \eta(x)\partial \overline{\eta(x)}\partial^4 \eta(x)}{\partial x\ \partial x\ \partial x^4} + 8\frac{\partial \eta(x)\partial^2 \overline{\eta(x)}\partial^3 \eta(x)}{\partial x\ \partial x^2\ \partial x^3}\right]\overline{\eta(x)}dx}{(C21\bar{U}_1 + C22\bar{U}_2)\int_0^1\frac{\partial \eta(x)}{\partial x}\overline{\eta(x)}dx + 2i\lambda\int_0^1\eta(x)\overline{\eta(x)}dx} +$$

$$\frac{\int_0^1\left[8\frac{\partial \overline{\eta(x)}\partial^2 \eta(x)\partial^3 \eta(x)}{\partial x\ \partial x^2\ \partial x^3} - 3C6\frac{\partial \eta(x)\partial \overline{\eta(x)}\partial^2 \eta(x)}{\partial x\ \partial x\ \partial x^2} + 8\frac{\partial \eta(x)\partial^2 \eta(x)\partial^3 \overline{\eta(x)}}{\partial x\ \partial x^2\ \partial x^3} - \frac{3}{2}C6\left(\frac{\partial \eta(x)}{\partial x}\right)^2\frac{\partial^2 \overline{\eta(x)}}{\partial x^2}\right]\overline{\eta(x)}dx}{(C21\bar{U}_1 + C22\bar{U}_2)\int_0^1\frac{\partial \eta(x)}{\partial x}\overline{\eta(x)}dx + 2i\lambda\int_0^1\eta(x)\overline{\eta(x)}dx}$$

$$K4 = \frac{\int_0^1\left[2\frac{\partial \Phi(x)\partial^4 \overline{\eta(x)}}{\partial x\ \partial x^4} + 4\frac{\partial^2 \Phi(x)\partial^3 \overline{\eta(x)}}{\partial x^2\ \partial 3} - C6\frac{\partial \Phi(x)\partial^2 \overline{\eta(x)}}{\partial x\ \partial x^2} - C6\frac{\partial \overline{\eta(x)}\partial^2 \Phi(x)}{\partial x\ \partial x^2}\right]\overline{\eta(x)}dx}{(C21\bar{U}_1 + C22\bar{U}_2)\int_0^1\frac{\partial \eta(x)}{\partial x}\overline{\eta(x)}dx + 2i\lambda\int_0^1\eta(x)\overline{\eta(x)}dx}$$

$$K5 = \frac{\int_0^1\left[3\frac{\partial^2 \eta(x)\partial^3 \eta(x)}{\partial x^2\ \partial x^3}\right]\overline{\eta(x)}dx}{(C21\bar{U}_1 + C22\bar{U}_2)\int_0^1\frac{\partial \eta(x)}{\partial x}\overline{\eta(x)}dx + 2i\lambda\int_0^1\eta(x)\overline{\eta(x)}dx}$$

To determine X(T1) and Y(T1), the solution of equations (97) and (98) is expressed in polar form:

$$Y(T1) = \frac{1}{2}\alpha y(T1)e^{i\beta y(T1)}\ \ and\ \ \overline{Y(T1)} = \frac{1}{2}\alpha y(T1)e^{-i\beta y(T1)} \quad (99)$$

$$X(T1) = \frac{1}{2}\alpha x(T1)e^{i\beta x(T1)}\ \ and\ \ \overline{Y(T1)} = \frac{1}{2}\alpha x(T1)e^{-i\beta x(T1)} \quad (100)$$

Preprints (www.preprints.org) | NOT PEER-REVIEWED | Posted: 6 October 2017 doi:10.20944/preprints201710.0030.v1

Peer-reviewed version available at Math. Comput. Appl. 2017, 22, 44; doi:10.3390/mca22040044

Substituting into the solvability condition and separating real and imaginary parts. The following set of modulation equation is formed:

$$0 = \frac{J2R\alpha y(T1)^2}{2}\cos(\psi 1) - \frac{d\alpha x(T1)}{dT1} - \frac{J2I\alpha y(T1)^2}{2}\sin(\psi 1)$$
$$0 = \frac{d\alpha y(T1)}{dT1} + \frac{K3R\alpha y(T1)^3}{4} - \frac{K5R\alpha y(T1)^2}{2}\cos(\psi 2) - \frac{K5I\alpha y(T1)^2}{2}\sin(\psi 2) - \frac{K4R\alpha y(T1)\alpha x(T1)}{2}\cos(\psi 1) - \frac{K4I\alpha y(T1)\alpha x(T1)}{2}\sin(\psi 1) \quad (111)$$
$$0 = \frac{J2R\alpha y(T1)^2}{2}\sin(\psi 1) - \alpha x(T1)\frac{d\beta x(T1)}{dT1} + \frac{J2I\alpha y(T1)^2}{2}\cos(\psi 1)$$
$$0 = \alpha y(T1)\frac{d\beta x(T1)}{dT1} + \frac{K5R\alpha y(T1)^2}{2}\sin(\psi 2) + \frac{K3I\alpha y(T1)^3}{4} - \frac{K5I\alpha y(T1)^2}{2}\cos(\psi 2) - \frac{K4I\alpha y(T1)\alpha x(T1)}{2}\cos(\psi 1) + \frac{K4R\alpha y(T1)\alpha x(T1)}{2}\sin(\psi 1)$$

Where:

$\psi 1 = \beta x(T1) - 2\beta y(T1) + \sigma T1$ and $\psi 2 = \beta y(T1) - \sigma T1$

$J2R, K3R, K4R, and\ K5R\ are\ the\ real\ part\ of\ J2, K3, K4\ and K5$
$J2I, K3I, K4I, and\ K5R\ are\ the\ real\ part\ of J2, K3, K4\ and K5$

Seeking for stationary solutions, $\alpha(x)' = \alpha(y)' = \psi 1' = \psi 2' = 0$ in modulation equations (112);

$$0 = \frac{J2R\alpha y(T1)^2}{2}\cos(\psi 1) - \frac{J2I\alpha y(T1)^2}{2}\sin(\psi 1)$$
$$0 = \frac{K3R\alpha y(T1)^3}{4} - \frac{K5R\alpha y(T1)^2}{2}\cos(\psi 2) - \frac{K5I\alpha y(T1)^2}{2}\sin(\psi 2) - \frac{K4R\alpha y(T1)\alpha x(T1)}{2}\cos(\psi 1) - \frac{K4I\alpha y(T1)\alpha x(T1)}{2}\sin(\psi 1)$$
$$0 = \frac{J2R\alpha y(T1)^2}{2}\sin(\psi 1) - \alpha x(T1)\sigma + \frac{J2I\alpha y(T1)^2}{2}\cos(\psi 1) \quad (113)$$
$$0 = \alpha y(T1)\sigma + \frac{K5R\alpha y(T1)^2}{2}\sin(\psi 2) + \frac{K3I\alpha y(T1)^3}{4} - \frac{K5I\alpha y(T1)^2}{2}\cos(\psi 2) - \frac{K4I\alpha y(T1)\alpha x(T1)}{2}\cos(\psi 1) + \frac{K4R\alpha y(T1)\alpha x(T1)}{2}\sin(\psi 1)$$

The linear solutions can be obtained by setting the coefficient of the nonlinear terms to zero. Therefore,

$$\alpha x(T1) = \alpha y(T1) = 0 \quad (114)$$

The nonlinear solutions can be obtained by solving for $\alpha x(T1)\ and\ \alpha y(T1)$ completely.

With the notations: $CS = cos\ (\psi 1)\ ,\ SS = sin(\psi 1)$

$\alpha x(T1)$ can be obtained by resolving the quartic frequency amplitude relation:

$$A.\alpha y(T1)^4 + B.\alpha y(T1)^2 + C = 0 \quad (115)$$

Where:

$A = \sigma^2 K3I^2 + \sigma^2 K3R^2 + CS^2 J2I^2 K4I^2 + CS^2 J2I^2 K4R^2 + CS^2 J2R^2 K4I^2 + CS^2 J2R^2 K4R^2 + J2I^2 K4I^2 SS^2 + J2I^2 K4R^2 SS^2 + J2R^2 K4I^2 SS^2 + J2R^2 K4R^2 SS^2 - 2CS.\sigma.K3I.K4I\sqrt{J2I^2 + J2R^2} - 2CS.\sigma.K3R.K4R\sqrt{J2I^2 + J2R^2} + 2\sigma.K3I.K4R.SS\sqrt{J2I^2 + J2R^2} - 2\sigma.K4I.K3R.SS\sqrt{J2I^2 + J2R^2}$

$B = -\left[4\sigma^2 K5I^2 + 4\sigma^2 K5R^2 - 8\sigma^3 K3I + 8CS.\ \sigma^2.K4I\sqrt{J2I^2 + J2R^2} - 8\ \sigma^2.K4R.SS.\sigma\sqrt{J2I^2 + J2R^2}\right]$

$C = 16\,\sigma^4$

The solution of the quartic equation (115) will produce four roots of $\alpha y(T1)$:

$$\alpha y(T1) = \pm\sqrt{-\frac{(B-\sqrt{B^2-4AC})}{2A}} \quad or \quad \alpha y(T1) = \pm\sqrt{-\frac{(B+\sqrt{B^2-4AC})}{2A}} \quad (116)$$

Preprints (www.preprints.org) | NOT PEER-REVIEWED | Posted: 6 October 2017 doi:10.20944/preprints201710.0030.v1

Peer-reviewed version available at Math. Comput. Appl. 2017, 22, 44; doi:10.3390/mca22040044

However, the acceptable solution for αy(T1) is the root of the quartic equation (115) that is real and positive [25-27]. The expression for estimating $\alpha x(T1)$ is defined in terms of αy(T1) as:

$$\alpha x(T1) = \frac{1}{\sigma}\left[\sqrt{\left(\frac{J2R\alpha y(T1)^2}{2}\right)^2 + \left(\frac{J2I\alpha y(T1)^2}{2}\right)^2}\right] \quad (117)$$

Considering the n-th values of αx(T1), αy(T1), βx(T1) and βy(T1) corresponding to the n-th modal functions and the n-th natural frequencies, the n-th solution of coupled problem is expressed as:

$$\bar{u}(x,t)_n = \alpha x(T1)_n \phi(x)_n \cos(\omega_n T0 + \beta x(T1)_n) + O(\varepsilon) \quad (118)$$
$$\bar{v}(x,t)_n = \alpha y(T1)_n \eta(x)_n \cos(\lambda_n T0 + \beta y(T1)_n) + O(\varepsilon) \quad (119)$$

Substituting: $T0 = t\,, T1 = \varepsilon t, \alpha x(T1)_n = \alpha x_n,\ \alpha y(T1)_n = \alpha y_n,\ \beta x(T1)_n = \psi 1_n + 2\beta y(T1)_n - \sigma_n T1,\ \beta y(T1)_n = \psi 2_n + \sigma_n T1$ and $\sigma_n T1 = \omega_n T0 - 2\lambda_n T0$

The first order approximate solution is expressed as:

$$\bar{u}(x,t) = \sum_{n=1}^{\infty} \alpha x_n |\phi(x)_n| \cos(\psi 1_n + 2\psi 2_n + 2t\omega_n - 2t\lambda_n + \varphi x_n) + O(\varepsilon) \quad (120)$$

$$\bar{v}(x,t) = \sum_{n=1}^{\infty} \alpha y_n |\eta(x)_n| \cos(\psi 2_n + t\omega_n - t\lambda_n + \varphi y_n) + O(\varepsilon) \quad (121)$$

Where the phase angles φx_n and φy_n are given by:

$$\tan(\varphi x_n) = \frac{Im\{\phi(x)_n\}}{Re\{\phi(x)_n\}},\ \tan(\varphi y_n) = \frac{Im\{\eta(x)_n\}}{Re\{\eta(x)_n\}}$$

Preprints (www.preprints.org) | NOT PEER-REVIEWED | Posted: 6 October 2017 doi:10.20944/preprints201710.0030.v1

Peer-reviewed version available at Math. Comput. Appl. 2017, 22, 44; doi:10.3390/mca22040044

3 Numerical Results

This section presents the numerical solutions of the nonlinear dynamics of a cantilever pipe conveying steady pressurized air/water two-phase flow. The axial linear natural frequencies for different flow velocities are estimated analytically from equation (61) while the transverse linear natural frequencies are estimated by solving equations (64) and (65) simultaneously with a numeric code written in Matlab.

Table 1: Summary of pipe and flow parameter

Parameter Name	Parameter Unit	Parameter Values
External Diameter	D_o (m)	0.0113772
Internal Diameter	D_i (m)	0.00925
Length	L (m)	0.1467
Pipe density	ρ_{pipe} (kg/m^3)	7800
Gas density	ρ_{Gas} (kg/m^3)	1.225
Water density	ρ_{Water} (kg/m^3)	1000
Tensile and compressive stiffness	EA (N)	7.24E+06
Bending stiffness	EI (N)	1.56E+03

Considering a simple system with β=0.2 and $\Pi 1$=100, $\Pi 0$= $\Pi 2$=0, a=$\alpha\Delta T$=0 for a single phase flow through the pipe, the natural frequency Argand diagram plot for the axial and transverse vibrations are presented in Figure 2 and Figure 3.

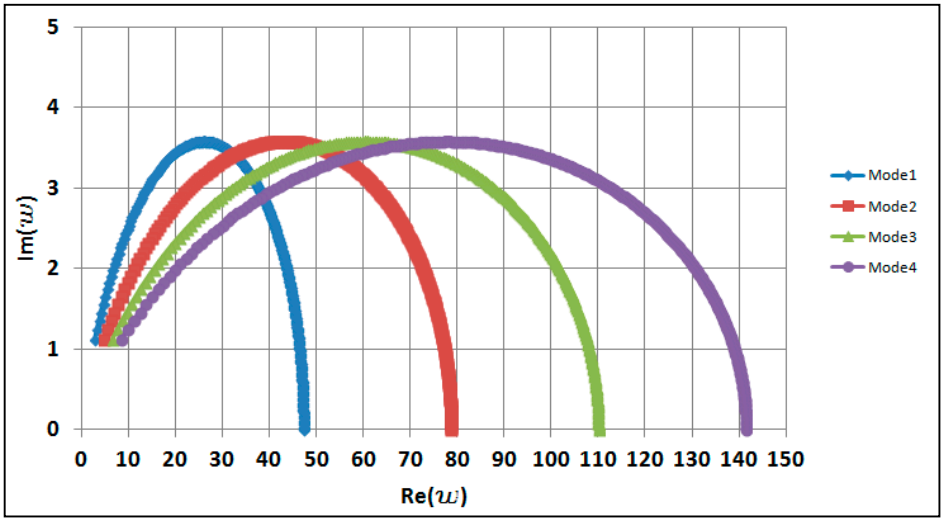

Figure 2: First four modes axial dimensionless complex frequency as a function of dimensionless single phase flow velocity

Preprints (www.preprints.org) | NOT PEER-REVIEWED | Posted: 6 October 2017 doi:10.20944/preprints201710.0030.v1

Peer-reviewed version available at Math. Comput. Appl. 2017, 22, 44; doi:10.3390/mca22040044

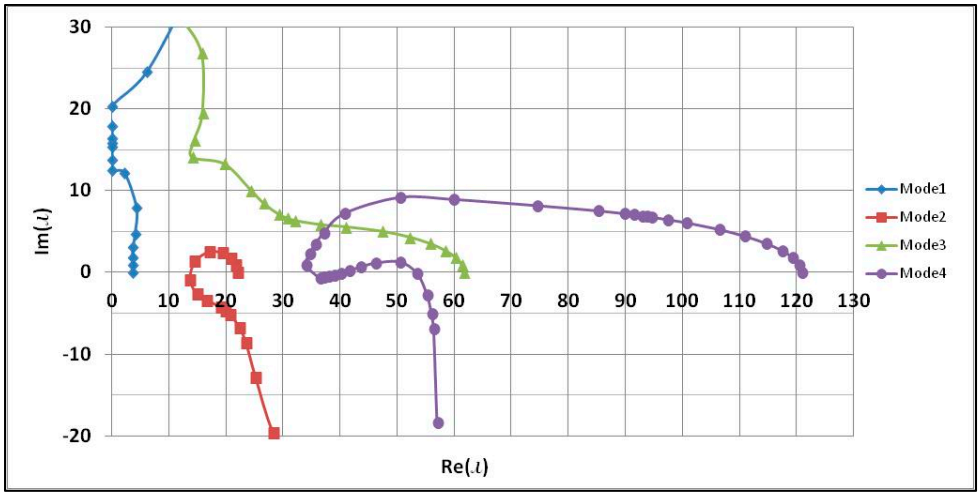

Figure 3: First four modes transverse dimensionless complex frequency as a function of dimensionless single phase flow velocity

The Argand diagram of the axial vibrations shows that as the fluid velocity tends towards the critical velocity; all the paths move towards the origin of the Argand diagram, while it can be seen for the transverse vibration that as the velocity attains higher values, the $Im(\omega)$ in the second mode of the system starts to diminish and in time becomes negative; Therefore, a Hopf bifurcation occurs at an approximate dimensionless velocity of 5.65 which is the critical velocity at which the systems becomes transversely unstable.

Table 2: Summary of the linear single phase solution's critical flow velocity

Fluid	Void Fraction	β Liquid	β Gas	Ψ Liquid	Ψ Gas	Critical velocity	
						Transverse	Axial
Single Phase	NA	0.2	0.0	1.0	0.0	5.653	14.149

The nonlinear behaviour of the pipe will be examined for both scenarios when there is coupling of the axial and transverse vibration and when both are uncoupled. The uncoupled nonlinear transverse frequency presented in Eq. (88) demonstrates a cubic nonlinear dependence of the uncoupled transverse frequencies on amplitude. The quartic expression presented in Eq. (115) relates the frequency detuning parameter for the coupled axial and transverse vibration with the amplitude. These expressions will be used to plot the frequency response curves for both the uncoupled and coupled scenarios and the nonlinear behaviour of the pipe as it conveys two-phase flow at a supercritical mixture velocity "flow velocity larger than the critical velocity"

3.1 Effects of two-phase flow on the dynamic behaviour of the pipe

The effect of two-phase flow is studied by considering the nonlinear response of the cantilever pipe as the void fraction of the two-phase flow changes. Similar to the single phase flow, the Argand diagram of the eigen-frequencies, , is used to find the critical velocities of the two-phase flow for the various void fractions (0.3, 0.4 and 0.5), with the corresponding slip ratios estimated from the Chisholm empirical relations presented in equations (32) to (36).

Preprints (www.preprints.org) | NOT PEER-REVIEWED | Posted: 6 October 2017 doi:10.20944/preprints201710.0030.v1

Peer-reviewed version available at Math. Comput. Appl. 2017, 22, 44; doi:10.3390/mca22040044

Table 3: Summary of the linear two-phase solution of critical flow velocities

Fluid	Void Fraction	β Liquid	β Gas	Ψ Liquid	Ψ Gas	Critical mixture velocity	
						Transverse	Axial
Two-phase	0.3	0.19998	0.00010	0.99948	0.00052	12.505	31.634
Two-phase	0.4	0.19997	0.00016	0.99918	0.00082	13.349	33.750
Two-phase	0.5	0.19995	0.00024	0.99878	0.00122	14.613	36.966

* Critical mixture velocity based on Hopf bifurcation of 2nd mode

Considering a supercritical mixture velocity of 15 and book keeping parameter (ε) of 0.1, the nonlinear frequency amplitude variations and coupled frequency response of the second mode, which is the stability determining mode in the linear sense, is plotted for various void fractions.

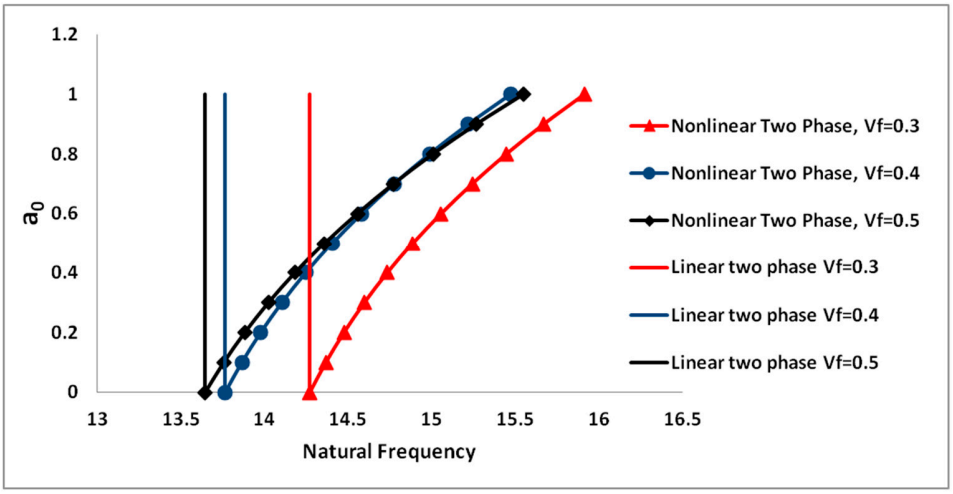

Figure 4: Nonlinear frequency –amplitude variations for various void fractions

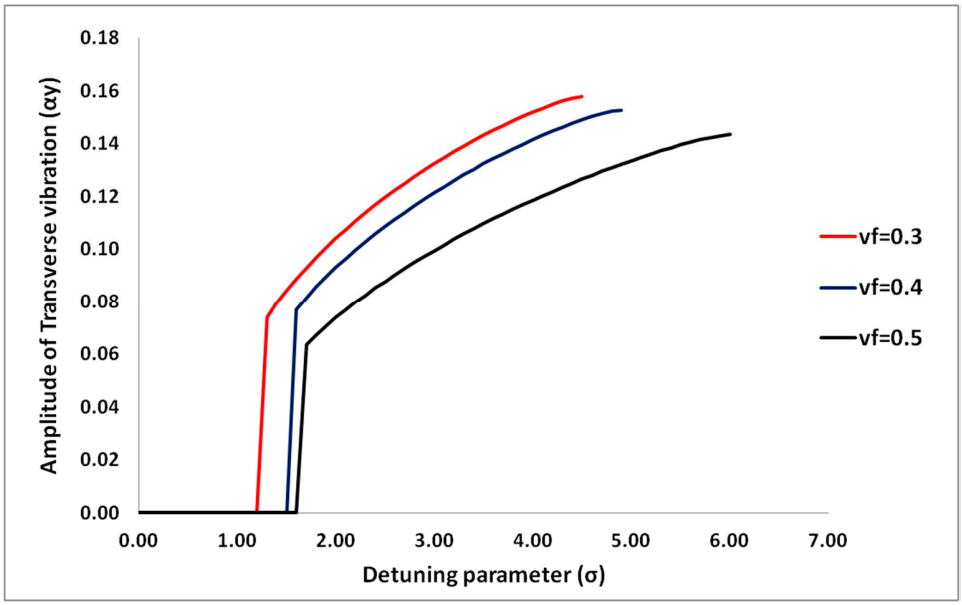

Figure 5: Nonlinear frequency response for various void fractions

Preprints (www.preprints.org) | NOT PEER-REVIEWED | Posted: 6 October 2017 doi:10.20944/preprints201710.0030.v1

Peer-reviewed version available at Math. Comput. Appl. 2017, 22, 44; doi:10.3390/mca22040044

It can be seen in Figure 4 that as the void fraction increases, the natural frequency reduces. A hardening nonlinear behaviour is observed in the dynamic response of the pipe for all the examined void fractions. As seen in Figure 5, as the detuning parameter is increasing, bifurcation is observed for the various void fractions examined. Also, it can be observed that the amplitude of the coupled transverse vibration is reducing as the void fraction increases.

3.1.1 Effects of temperature difference on the dynamic behaviour

The effect of temperature differences on a cantilever pipe conveying two-phase flow is studied by considering the nonlinear response of the cantilever pipe as the temperature differences of the two-phase flow with void fraction of 0.3 changes. Similar to the single phase flow, the Argand diagram of the eigen-frequencies, , is used to find the critical velocities of the two-phase flow for the various temperature differences (0, 40 and 50), with the corresponding slip ratios estimated from the Chisholm empirical relations presented in equations (32) to (36).

Table 4: Summary of the linear two-phase solution of critical flow velocities for varying temperature difference

Parameter	Void Fraction	Thermal expansivity α	Critical mixture velocity	
			Transverse*	Axial
DT=0	0.3	0.002	12.505	31.634
DT=40	0.3	0.002	9.253	31.634
DT=50	0.3	0.002	8.237	31.634

* Critical mixture velocity based on Hopf bifurcation of 2nd mode

Considering a supercritical mixture velocity of 15 and book keeping parameter (ε) of 0.1, the nonlinear frequency amplitude variations and coupled frequency response of the second mode, which is the stability determining mode in the linear sense, is plotted for various temperature differences.

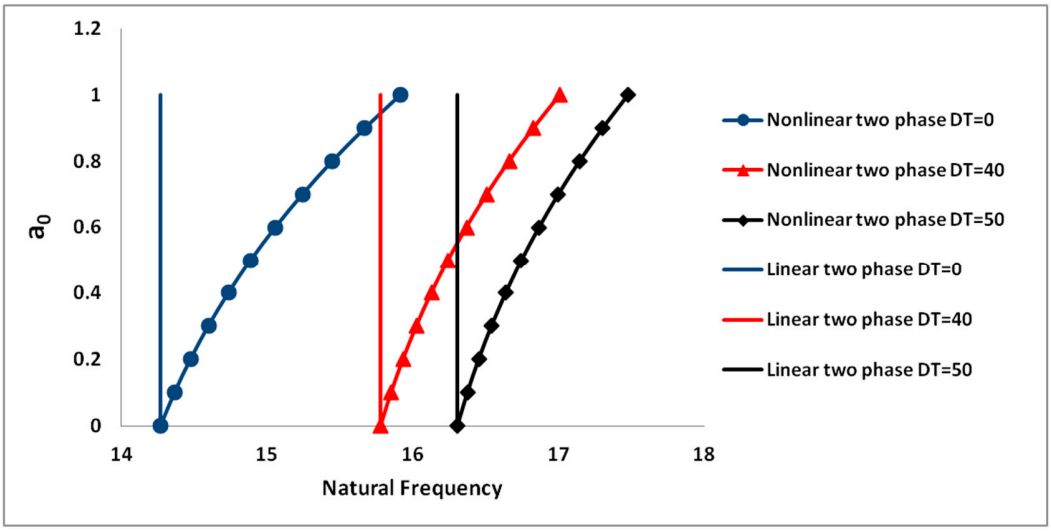

Figure 6: Nonlinear frequency –amplitude variations for various temperature differences

Preprints (www.preprints.org) | NOT PEER-REVIEWED | Posted: 6 October 2017 doi:10.20944/preprints201710.0030.v1

Peer-reviewed version available at Math. Comput. Appl. 2017, 22, 44; doi:10.3390/mca22040044

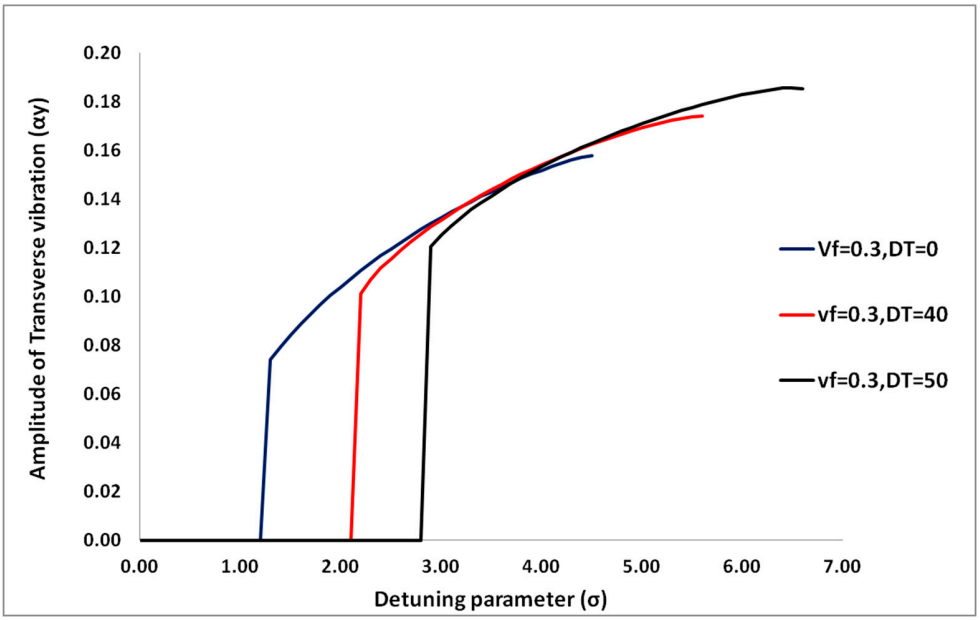

Figure 7: Nonlinear frequency response for various temperature differences

It can be seen in Figure 6 that as the temperature difference increases, the natural frequency increases. A hardening nonlinear behaviour is observed in the dynamic response of the pipe for all the examined temperature differences. As seen in Figure 7, as the detuning parameter is increasing, bifurcation is observed for the various temperature difference examined. Also, it can be observed that the increase in temperature difference did not create significant changes in amplitude of the coupled transverse vibration.

3.1.2 Effects of flow pressure on the dynamic behaviour

The effect of pressurization on a cantilever pipe conveying two-phase flow is studied by considering the nonlinear response of the cantilever pipe as the pressurization of the two-phase flow with void fraction of 0.3 changes. Similar to the single phase flow, the Argand diagram of the eigen-frequencies, , is used to find the critical velocities of the two-phase flow for the various pressures (0, 5 and 10), with the corresponding slip ratios estimated from the Chisholm empirical relations presented in equations (32) to (36).

Table 5: Summary of the linear two-phase solution of critical flow velocities for varying pressurization

Parameter	Void Fraction	Critical mixture velocity	
		Transverse *	Axial
Π2 = 0	0.3	12.505	31.634
Π2 = 5	0.3	10.596	31.634
Π2 = 10	0.3	8.237	31.634

* Critical mixture velocity based on Hopf bifurcation of 2nd mode

Preprints (www.preprints.org) | NOT PEER-REVIEWED | Posted: 6 October 2017 doi:10.20944/preprints201710.0030.v1

Peer-reviewed version available at Math. Comput. Appl. 2017, 22, 44; doi:10.3390/mca22040044

Considering a supercritical mixture velocity of 15 and book keeping parameter (ε) of 0.1, the nonlinear frequency amplitude variations and coupled frequency response of the second mode which is the stability determining mode in the linear sense, is plotted for various pressures.

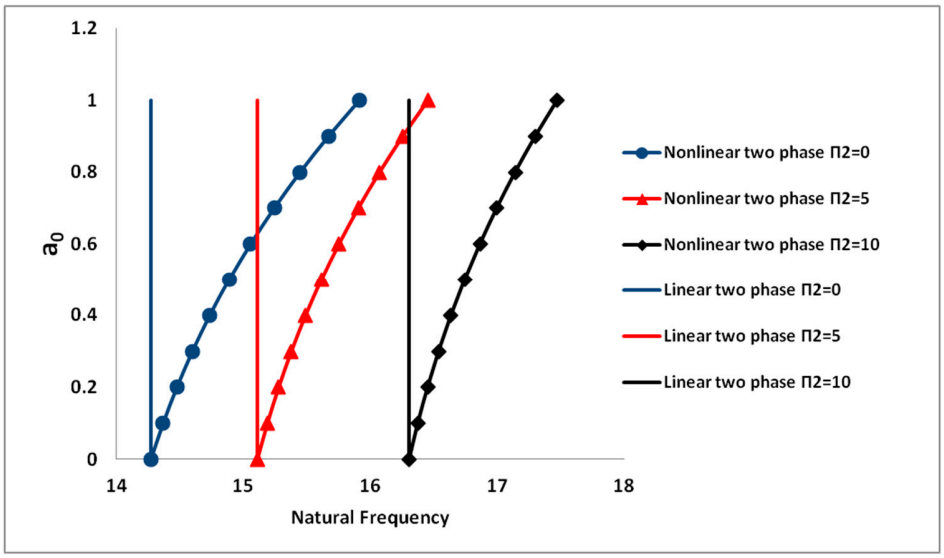

Figure 8: Nonlinear frequency –amplitude variations for various pressures

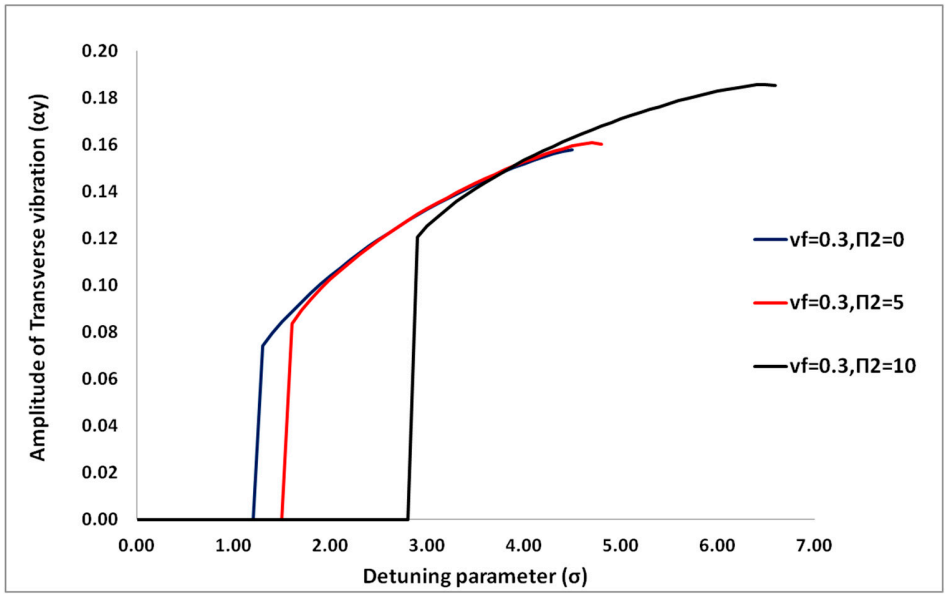

Figure 9: Nonlinear frequency response for various pressures

It can be seen in Figure 8 that as the pressure increases, the natural frequency increases. A hardening nonlinear behaviour is observed in the dynamic response of the pipe for all the examined pressures. As seen in Figure 9, as the detuning parameter is increasing, bifurcation is observed for the various pressures examined. Also, it can be observed that the increasing the pressure did not create significant changes in amplitude of the coupled transverse vibration.

Preprints (www.preprints.org) | NOT PEER-REVIEWED | Posted: 6 October 2017 doi:10.20944/preprints201710.0030.v1

Peer-reviewed version available at Math. Comput. Appl. 2017, 22, 44; doi:10.3390/mca22040044

3.1.3 Effects of top tension on the dynamic behaviour

The effect of top tension on a cantilever pipe conveying two-phase flow is studied by considering the nonlinear response of the cantilever pipe for a situation with no top tension, tensioning value of 5 and compressing value of 5, with a two-phase flow of void fraction of 0.3. Similar to the single phase flow, the Argand diagram of the eigen-frequencies, , is used to find the critical velocities of the two-phase flow for the various tensioning values, the corresponding slip ratios are estimated from the Chisholm empirical relations presented in equations (32) to (36).

Table 6: Summary of the linear two-phase solution of critical flow velocities for varying top tensions

Parameter	Void Fraction	Critical velocity	
		Transverse*	Axial
$\Pi 0 = 0$	0.3	12.505	31.634
$\Pi 0 = 5$	0.3	14.155	31.634
$\Pi 0 = -5$	0.3	10.596	31.634

* Critical mixture velocity based on Hopf bifurcation of 2nd mode

Considering a supercritical mixture velocity of 15 and book keeping parameter (ε) of 0.1, the nonlinear frequency amplitude variations and coupled frequency response of the second mode which is the stability determining mode in the linear sense, is plotted for the top tensions.

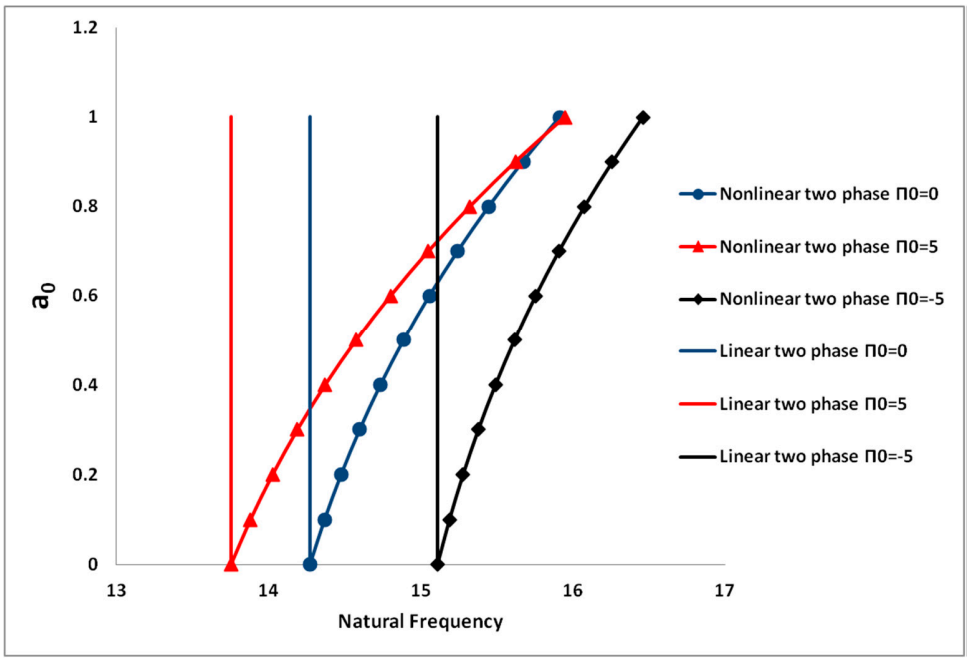

Figure 10: Nonlinear frequency –amplitude variations for various top tensions

Preprints (www.preprints.org) | NOT PEER-REVIEWED | Posted: 6 October 2017 doi:10.20944/preprints201710.0030.v1

Peer-reviewed version available at Math. Comput. Appl. 2017, 22, 44; doi:10.3390/mca22040044

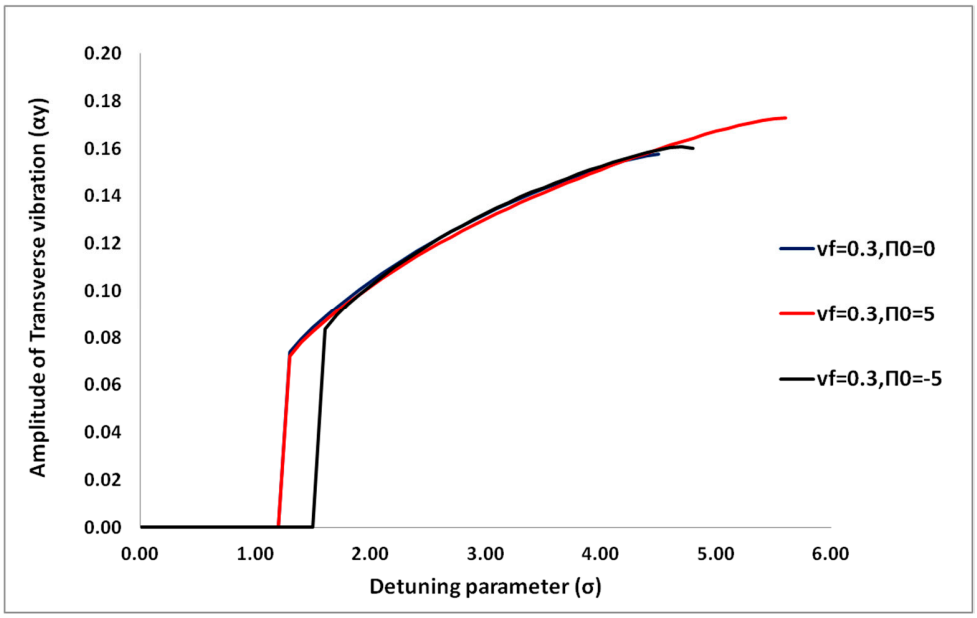

Figure 11: Nonlinear frequency response for various top tensions

It can be seen in Figure 10 that the tensioning top load reduces the natural frequency increases while a compressing top load increases the natural frequency. A hardening nonlinear behaviour is observed in the dynamic response of the pipe for all the examined cases. As seen in Figure 11, as the detuning parameter is increasing, bifurcation is observed for the various pressures examined. Also, it can be observed that the top tensions did not create significant changes in amplitude of the coupled transverse vibration.

3.2 Time History and Phase Plots

Equations (91), (92), (120), and (121) are the first order approximate solutions of the transverse and axial displacement of the uncoupled and coupled vibration of the pipe. The time trace/history and phase plots of the 2^{nd} mode of the uncoupled and coupled vibrations are studied for various void fractions (0.3, 0.4 and 0.5) considering a post critical flow mixture velocity of 15 and presented in Figures 12 to 23.

The uncoupled response of the transverse vibrations as shown in Figures 12, 16 and 20 for the various void fractions looks similar, they all shows that the uncoupled transverse vibrations exhibits an oscillation that converges to a limit cycle with time. With initial amplitudes greater that the amplitudes of the limit cycles; hence, a positive initial damping is observed and the amplitudes decays until it attains the limit cycles as shown in the phase plot with a set of concentric circles inside the phase trajectories. Contrary to this, the uncoupled axial vibration as shown in Figures, 13, 17 and 21 is observed to exhibit uniform periodic oscillations, which traces out as a closed orbit in the phase plots. The amplitudes of the displacements are observed to reduce as the void fraction is increasing.

As a result of the coupling between the axial and the transverse vibration, both the coupled transverse and axial solutions as shown in Figures 14, 15, 18, 19, 22 and 23, exhibits uniform periodic oscillations, which trace out as a closed orbit in the phase plots. The amplitudes of the coupled displacements are observed to reduce as the void fraction is increasing.

Preprints (www.preprints.org) | NOT PEER-REVIEWED | Posted: 6 October 2017 doi:10.20944/preprints201710.0030.v1

Peer-reviewed version available at Math. Comput. Appl. 2017, 22, 44; doi:10.3390/mca22040044

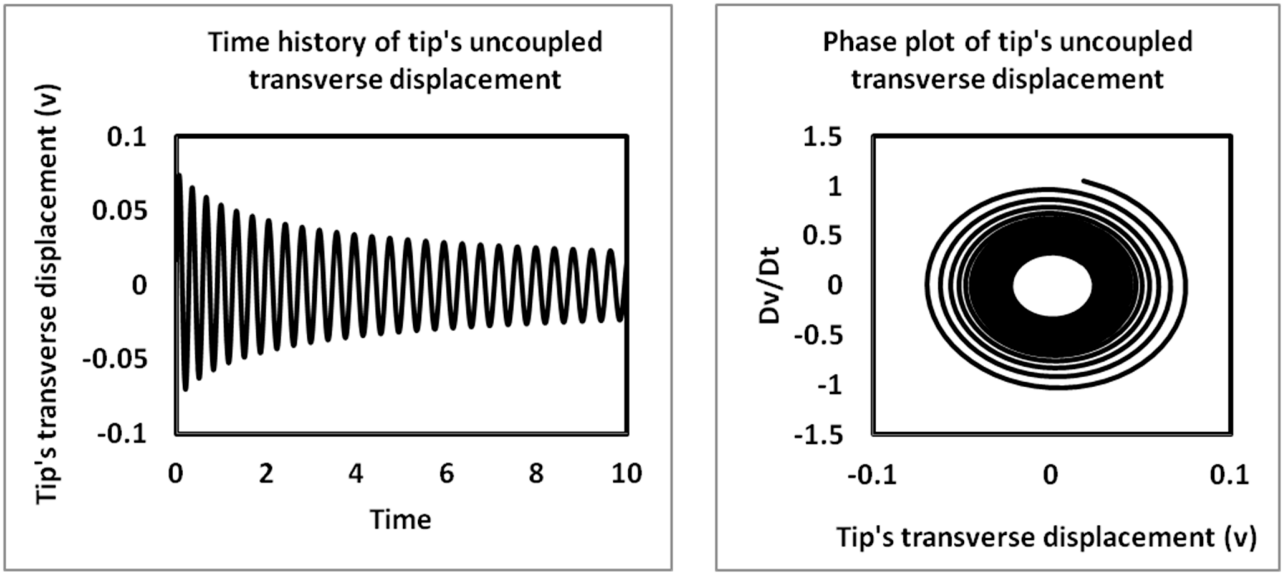

Figure 12: Time history and phase plots of uncoupled transverse vibrations of the tip of a cantilever pipe conveying two-phase flow of void fraction of 0.3

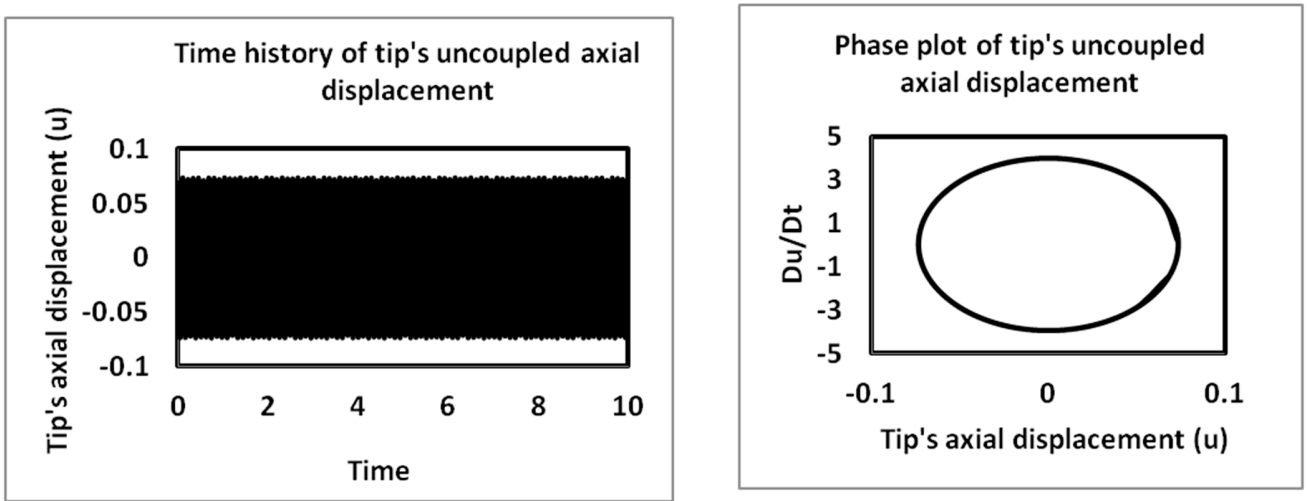

Figure 13: Time history and phase plots of uncoupled axial vibrations of the tip of a cantilever pipe conveying two-phase flow of void fraction of 0.3

Preprints (www.preprints.org) | NOT PEER-REVIEWED | Posted: 6 October 2017 doi:10.20944/preprints201710.0030.v1

Peer-reviewed version available at Math. Comput. Appl. 2017, 22, 44; doi:10.3390/mca22040044

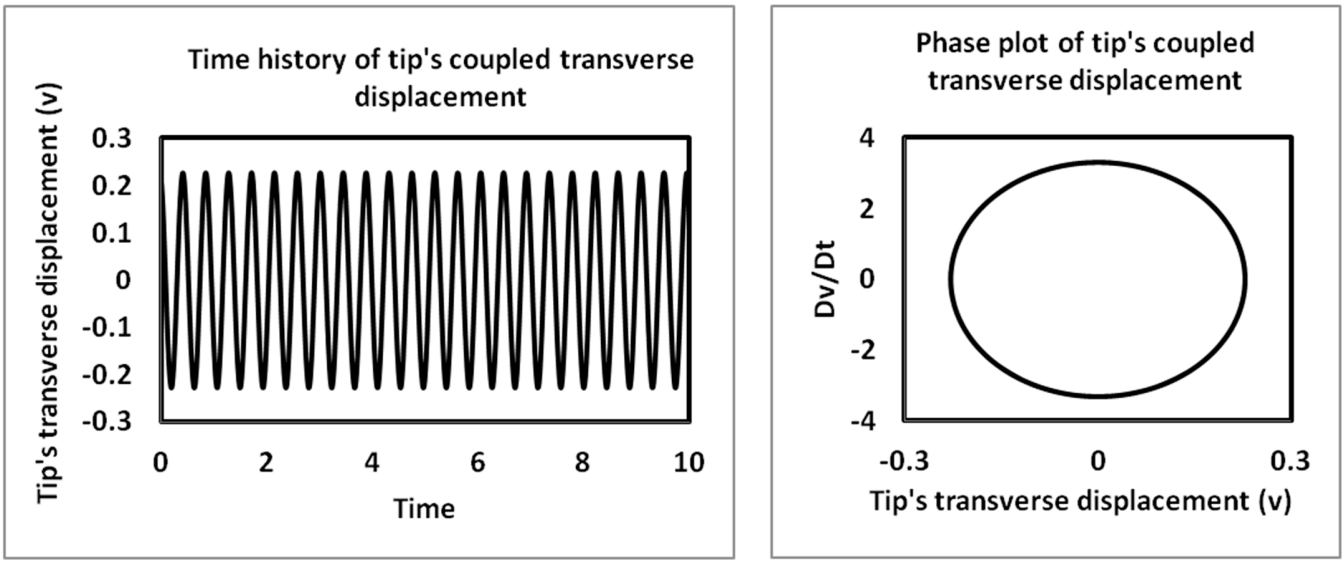

Figure 14: Time history and phase plots of coupled transverse vibrations of the tip of a cantilever pipe conveying two-phase flow of void fraction of 0.3, σ of 2.0

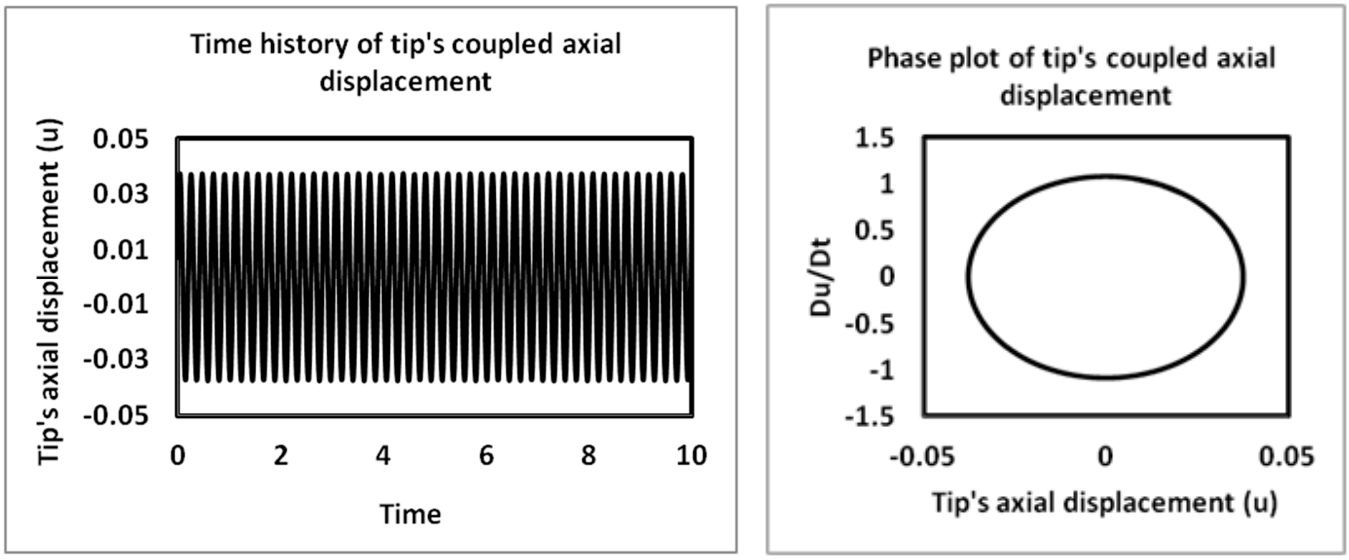

Figure 15: Time history and phase plots of coupled axial vibrations of the tip of a cantilever pipe conveying two-phase flow of void fraction of 0.3, σ of 2.0

Preprints (www.preprints.org) | NOT PEER-REVIEWED | Posted: 6 October 2017 doi:10.20944/preprints201710.0030.v1

Peer-reviewed version available at Math. Comput. Appl. 2017, 22, 44; doi:10.3390/mca22040044

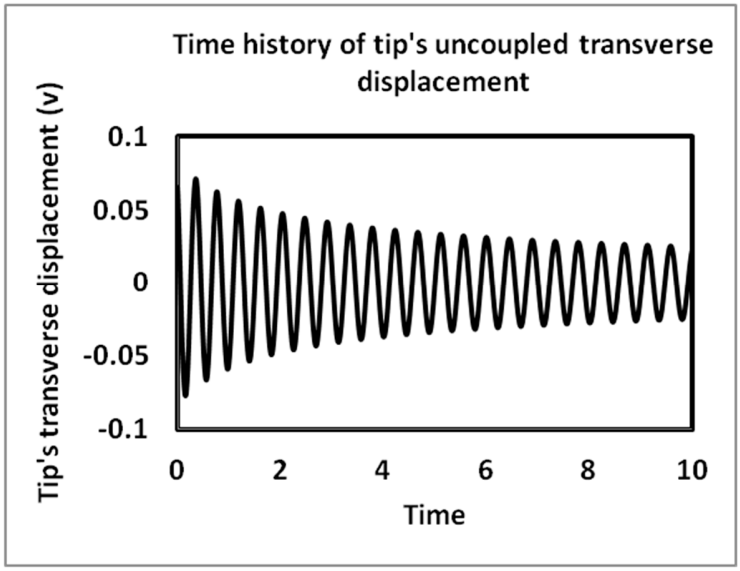

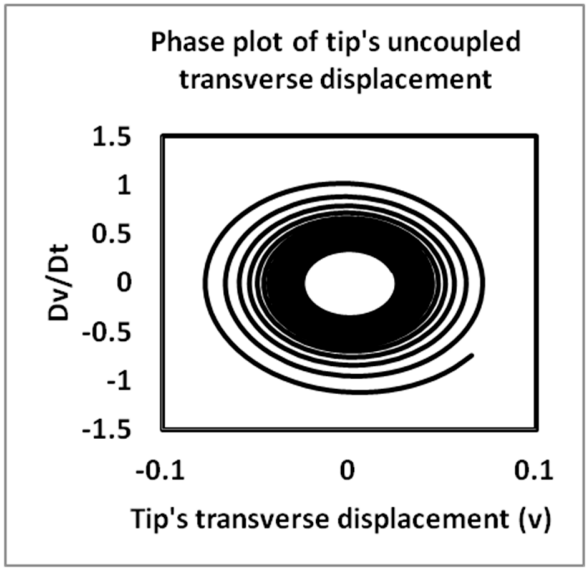

Figure 16: Time history and phase plots of uncoupled transverse vibrations of the tip of a cantilever pipe conveying two-phase flow of void fraction of 0.4

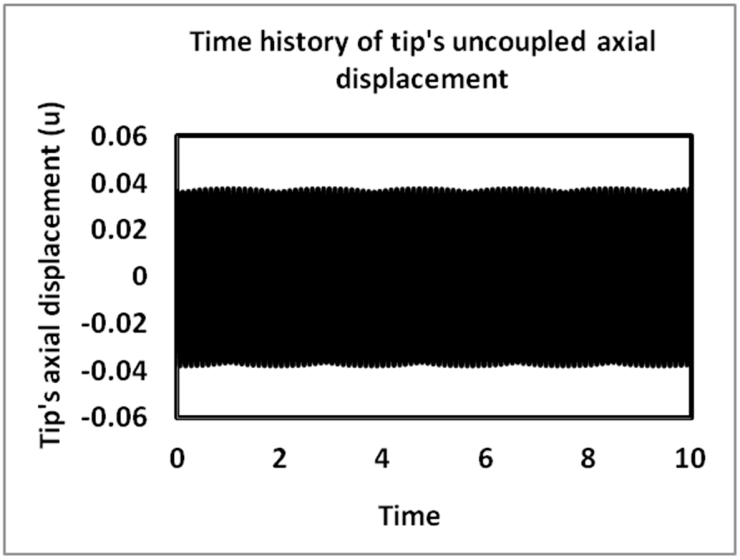

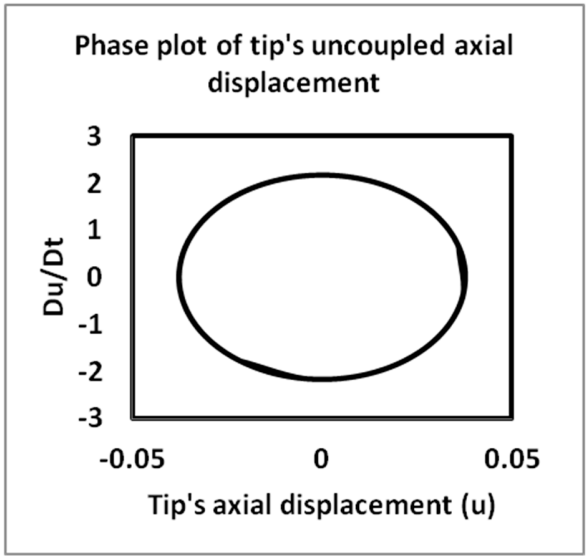

Figure 17: Time history and phase plots of uncoupled axial vibrations of the tip of a cantilever pipe conveying two-phase flow of void fraction of 0.4

Preprints (www.preprints.org) | NOT PEER-REVIEWED | Posted: 6 October 2017 doi:10.20944/preprints201710.0030.v1

Peer-reviewed version available at Math. Comput. Appl. 2017, 22, 44; doi:10.3390/mca22040044

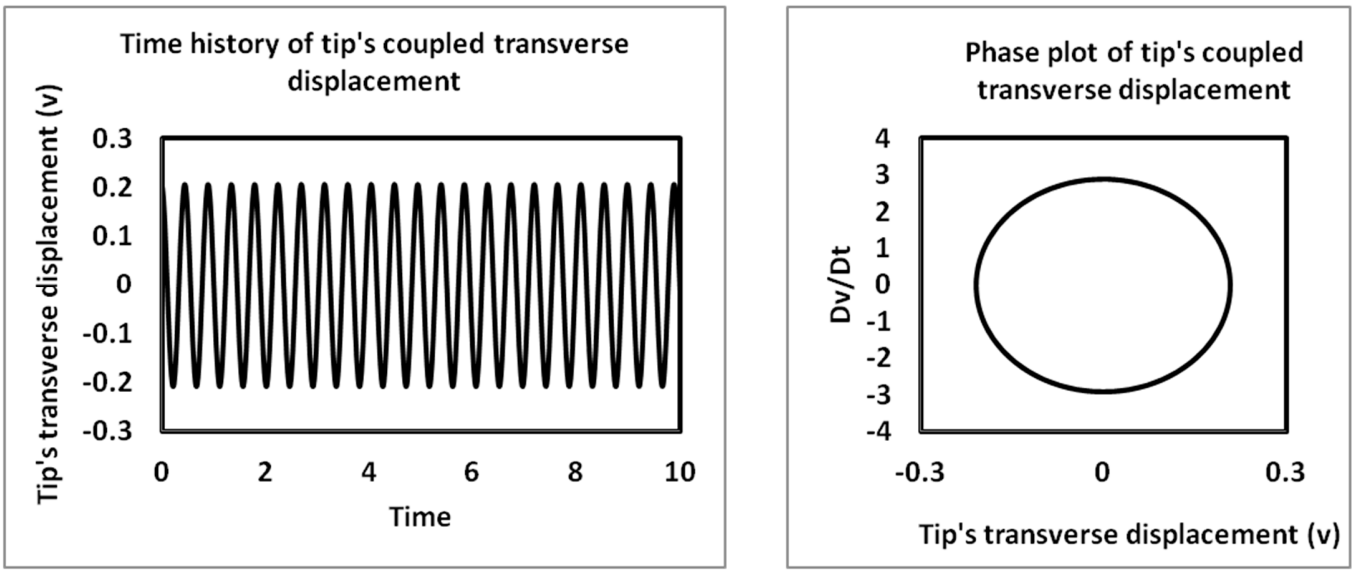

Figure 18: Time history and phase plots of coupled transverse vibrations of the tip of a cantilever pipe conveying two-phase flow of void fraction of 0.4, σ of 2.0

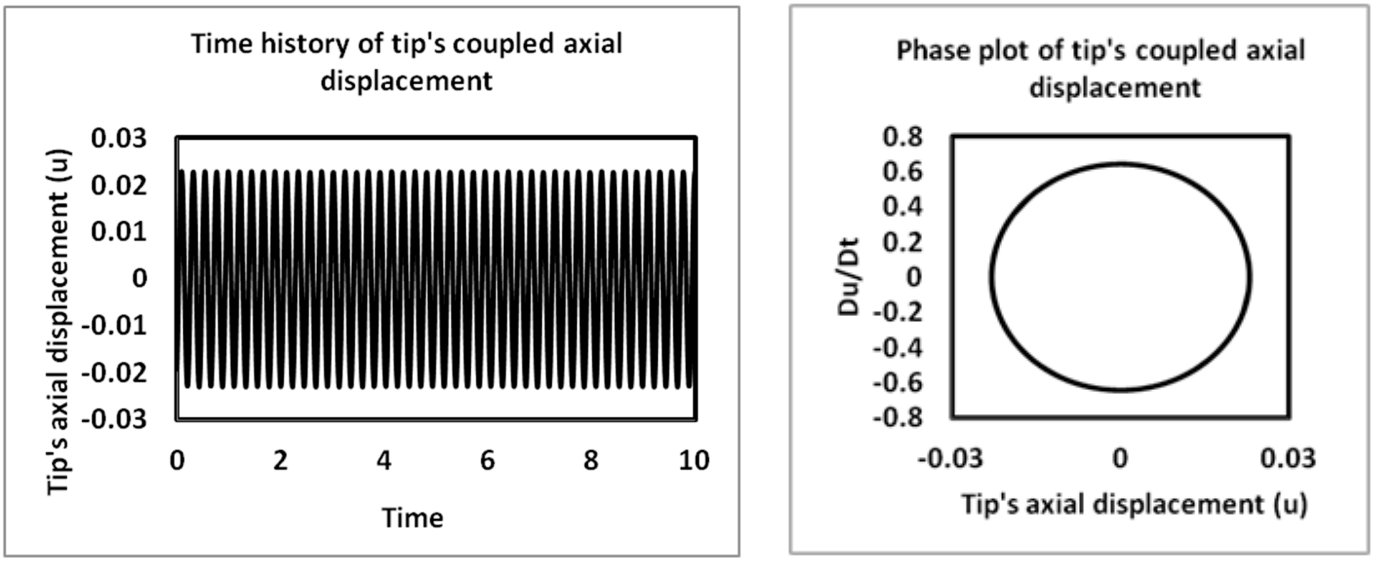

Figure 19: Time history and phase plots of coupled axial vibrations of the tip of a cantilever pipe conveying two-phase flow of void fraction of 0.4, σ of 2.0

Preprints (www.preprints.org) | NOT PEER-REVIEWED | Posted: 6 October 2017 doi:10.20944/preprints201710.0030.v1

Peer-reviewed version available at Math. Comput. Appl. 2017, 22, 44; doi:10.3390/mca22040044

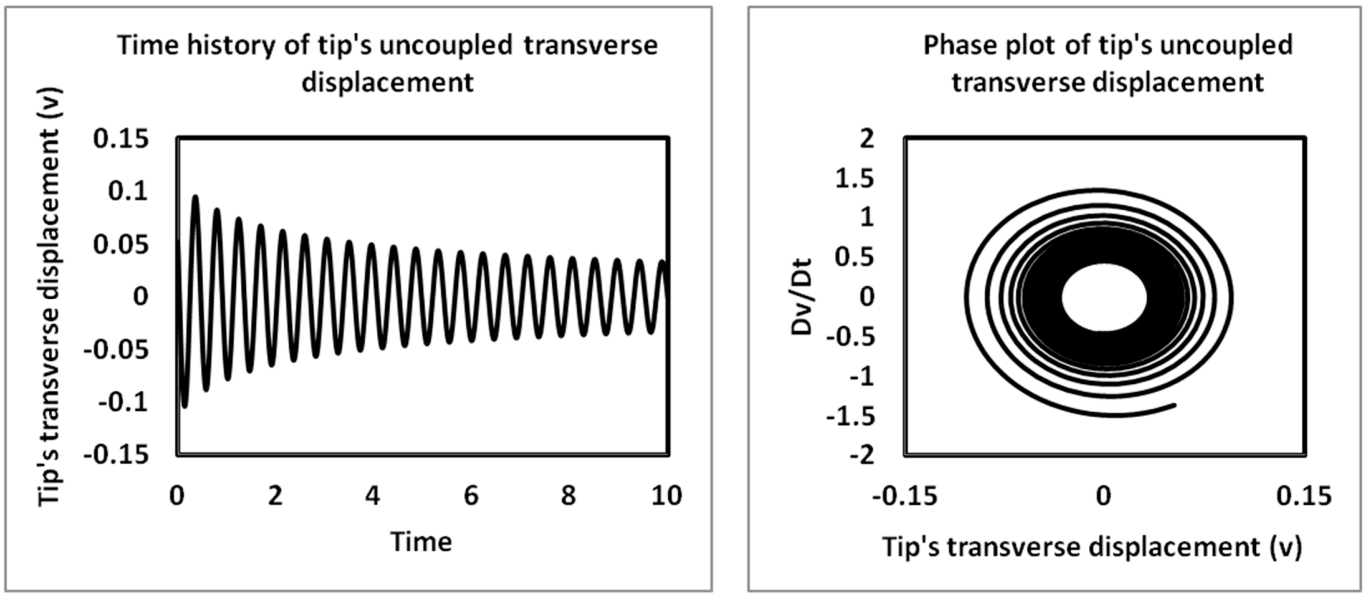

Figure 20: Time history and phase plots of uncoupled transverse vibrations of the tip of a cantilever pipe conveying two-phase flow of void fraction of 0.5

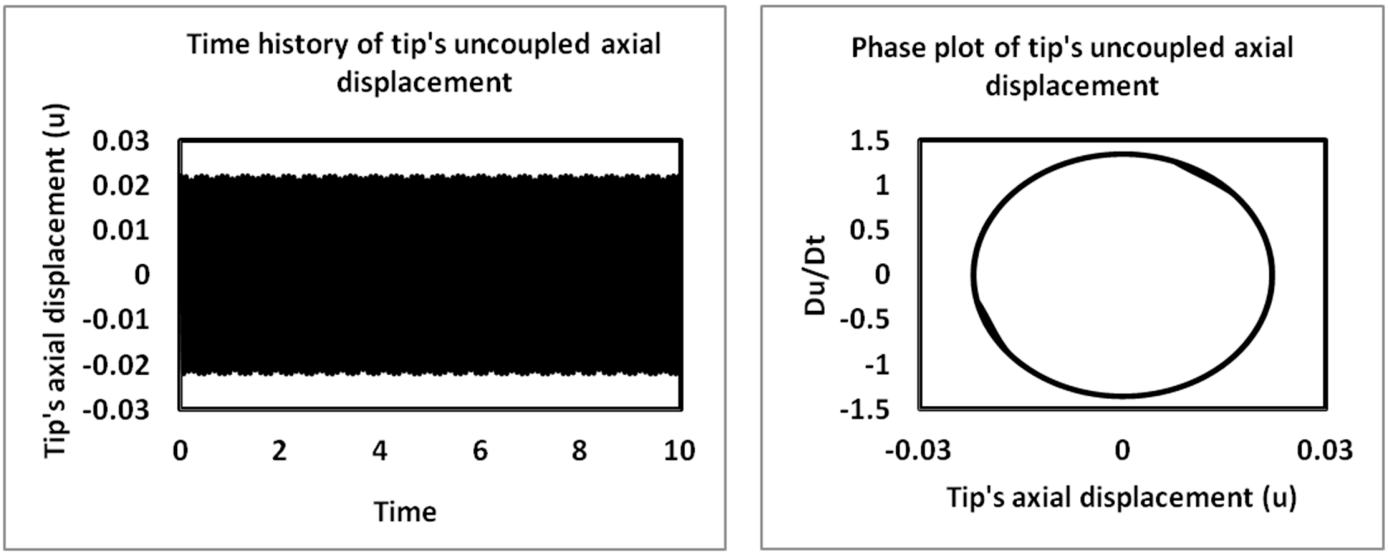

Figure 21: Time history and phase plots of uncoupled axial vibrations of the tip of a cantilever pipe conveying two-phase flow of void fraction of 0.5

Preprints (www.preprints.org) | NOT PEER-REVIEWED | Posted: 6 October 2017 doi:10.20944/preprints201710.0030.v1

Peer-reviewed version available at Math. Comput. Appl. 2017, 22, 44; doi:10.3390/mca22040044

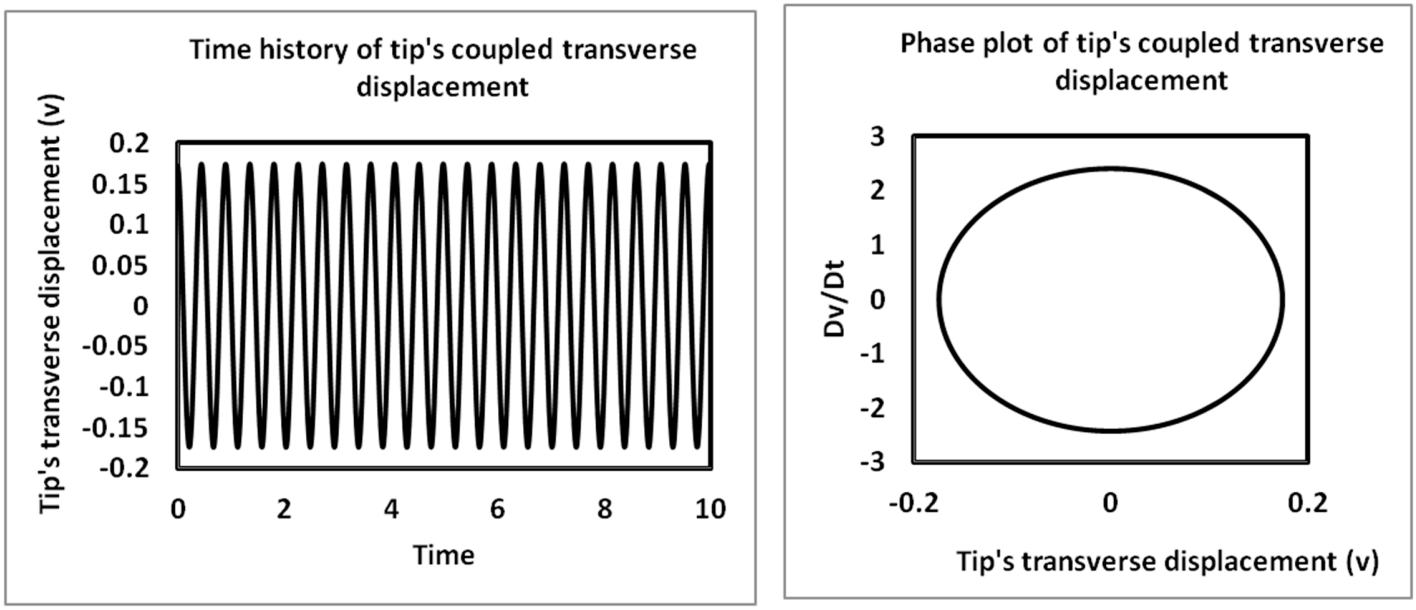

Figure 22: Time history and phase plots of coupled transverse vibrations of the tip of a cantilever pipe conveying two-phase flow of void fraction of 0.5, σ of 2.0

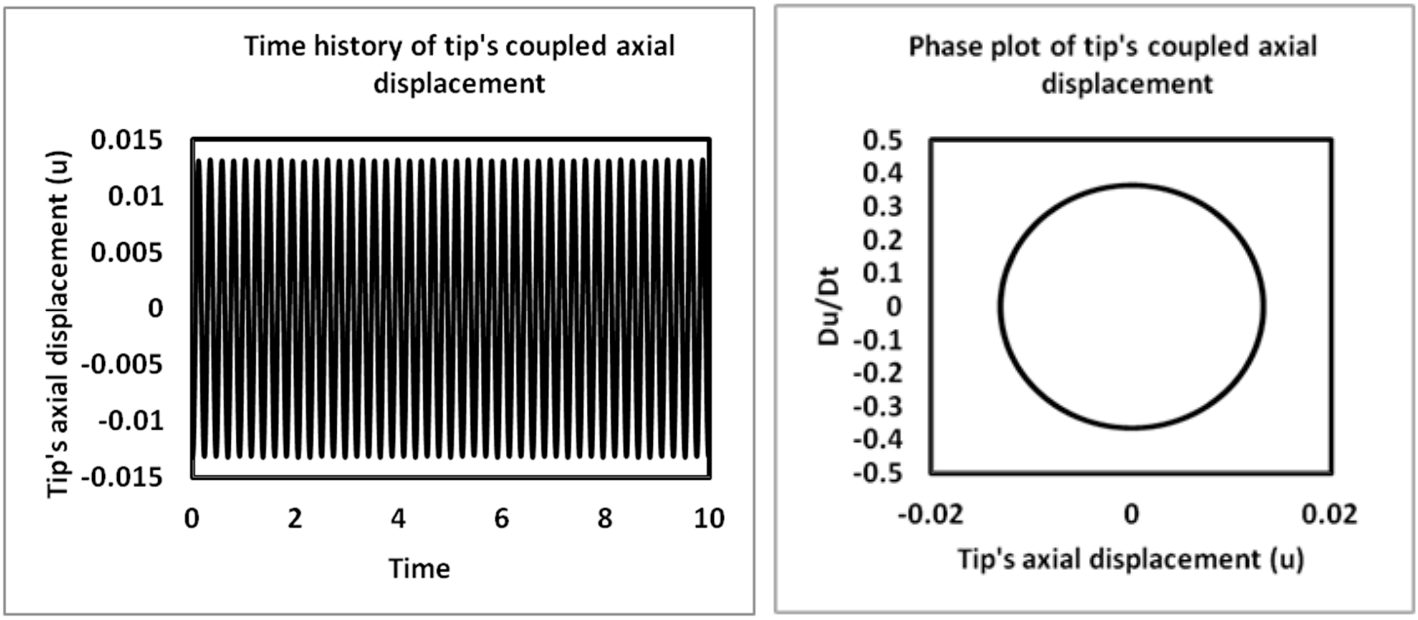

Figure 23: Time history and phase plots of uncoupled axial vibrations of the tip of a cantilever pipe conveying two-phase flow of void fraction of 0.5, σ of 2.0

Preprints (www.preprints.org) | NOT PEER-REVIEWED | Posted: 6 October 2017 doi:10.20944/preprints201710.0030.v1

Peer-reviewed version available at Math. Comput. Appl. 2017, 22, 44; doi:10.3390/mca22040044

4 Conclusion

This study examines the dynamic behaviour of a cantilever pipe conveying two-phase flow. Taking into consideration the extensible theory, nonlinear equations of motion and boundary conditions were obtained using Hamilton's principle. The equations were made to be non-dimensional so as to remove the dependence on geometric and dimensional parameters. Using the method multiple scale perturbation technique, natural frequencies, mode shapes and first order approximate solutions of the steady state response of the pipes were obtained. From the analytical assessment, it was observed that a 1:2 coupling exist between the axial and the transverse vibration of the pipe.

The critical flow mixture velocity for various void fractions were obtained from the Argand diagram plot of the eigen-frequencies, it was observed that the critical velocities increases as the void fraction increases. The investigation of the uncoupled nonlinear dynamic behaviour of the pipe as it conveys two-phase flow at a super critical mixture velocity reveals that the system exhibits a nonlinear hardening behaviour. As a result of the dynamic analysis, it has been observed that for a two-phase flow, increase in the void fractions reduces the natural frequency and the coupled amplitude of the system. Also, increase in temperature difference, increase in pressure and the presence of top tension were observed to increase the natural frequencies without a significant alteration in the coupled amplitude of the system while compression load at the top was observed to reduce the natural frequencies which out a significant change in the coupled amplitude of the system.

APPENDIX

Techniques for completely solving for $\alpha x(T1)\ and\ \alpha y(T1)$

Using Trigonometry identities,

$$
\begin{aligned}
&R\,sin(\psi+\theta) = Rcos(\theta)sin(\psi) + Rsin(\theta)cos(\psi)\\
&R\,cos(\psi+\theta) = Rcos(\theta)cos(\psi) - Rsin(\theta)sin(\psi)\\
&R\,sin(\psi-\theta) = Rcos(\theta)sin(\psi) - Rsin(\theta)cos(\psi)\\
&R\,cos(\psi-\theta) = Rcos(\theta)cos(\psi) + Rsin(\theta)sin(\psi) \qquad (A1)
\end{aligned}
$$

Equation (113a) and (113c) can be rewritten as:

$$0 = R1\sin(\psi 1+\theta 1) \qquad (A2)$$

$$\alpha x(T1)\sigma = R1\cos(\psi 1+\theta 1) \qquad (A3)$$

$$\tan(\theta 1) = \frac{J2I}{J2R},\ R1 = \sqrt{\left(\frac{J2R\alpha y(T1)^2}{2}\right)^2 + \left(\frac{J2I\alpha y(T1)^2}{2}\right)^2} \qquad (A4)$$

From;

$$(\sin(\psi 1+\theta 1))^2 + (\cos(\psi 1+\theta 1))^2 = 1 \qquad (A5)$$

$$\alpha x(T1) = \pm\sqrt{\frac{R1^2}{\sigma^2}} \qquad (A6)$$

Preprints (www.preprints.org) | NOT PEER-REVIEWED | Posted: 6 October 2017 doi:10.20944/preprints201710.0030.v1

Peer-reviewed version available at Math. Comput. Appl. 2017, 22, 44; doi:10.3390/mca22040044

From equation (A2) or (A4);

$$\psi 1 = \frac{\pi}{2} + \theta 1 \qquad (A7)$$

Equation (113b) and (113d) can be rewritten as:

$$\frac{K3I\alpha y(T1)^3}{4} + \alpha y(T1)\sigma - \frac{K4I\alpha x(T1)\alpha y(\mathrm{T1})\cos(\psi 1)}{2} + \frac{K4R\alpha x(T1)\alpha y(\mathrm{T1})\sin(\psi 1)}{2} = R2\sin(\psi 2 - \theta 2) \qquad (A8)$$

$$\frac{K3R\alpha y(T1)^3}{4} - \frac{K4R\alpha x(T1)\alpha y(\mathrm{T1})\cos(\psi 1)}{2} - \frac{K4I\alpha x(T1)\alpha y(\mathrm{T1})\sin(\psi 1)}{2} = R2\cos(\psi 2 - \theta 2) \qquad (A9)$$

$$\tan(\theta 2) = \frac{K5I}{K5R},\ R2 = \sqrt{\left(\frac{K5I\alpha y(T1)^2}{2}\right)^2 + \left(\frac{K5R\alpha y(T1)^2}{2}\right)^2} \qquad (A10)$$

From equation (A8) and (A9)

$$\psi 2 = \theta 2 - \tan^{-1}\left[\frac{K3I\alpha y(T1)^2 - 2K4I\alpha x(T1)\cos(\psi 1) + 2K4R\alpha x(T1)\sin(\psi 1) + 4\sigma}{-K3R\alpha y(T1)^2 + 2K4R\alpha x(T1)\cos(\psi 1) + 2K4I\alpha x(T1)\sin(\psi 1)}\right] \qquad (A11)$$

Let

$$\alpha x(T1) = \frac{R1}{\sigma}, \qquad CS = cos\ (\psi 1), \qquad SS = sin(\psi 1) \qquad (A12)$$

From;

$$(\sin(\psi 2 - \theta 2))^2 + (\cos(\psi 2 - \theta 2))^2 = 1 \qquad (A13)$$

Substituting the expressions of R1 and R2 from equations (A4) and (A10) respectively, a quartic equation in terms of $\alpha y(T1)$ is obtained as:

$$A.\alpha y(T1)^4 + B.\alpha y(T1)^2 + C = 0 \qquad (A14)$$

Where:

$A = \sigma^2\mathrm{K3I}^2 + \sigma^2\mathrm{K3R}^2 + \mathrm{CS}^2\mathrm{J2I}^2\mathrm{K4I}^2 + \mathrm{CS}^2\mathrm{J2I}^2\mathrm{K4R}^2 + \mathrm{CS}^2\mathrm{J2R}^2\mathrm{K4I}^2 + \mathrm{CS}^2\mathrm{J2R}^2\mathrm{K4R}^2 + \mathrm{J2I}^2\mathrm{K4I}^2\mathrm{SS}^2 + \mathrm{J2I}^2\mathrm{K4R}^2\mathrm{SS}^2 + \mathrm{J2R}^2\mathrm{K4I}^2\mathrm{SS}^2 + \mathrm{J2R}^2\mathrm{K4R}^2\mathrm{SS}^2 - 2\mathrm{CS}.\sigma.\mathrm{K3I}.\mathrm{K4I}\sqrt{\mathrm{J2I}^2 + \mathrm{J2R}^2} - 2\mathrm{CS}.\sigma.\mathrm{K3R}.\mathrm{K4R}\sqrt{\mathrm{J2I}^2 + \mathrm{J2R}^2} + 2\,\sigma.\mathrm{K3I}.\mathrm{K4R}.\mathrm{SS}\sqrt{\mathrm{J2I}^2 + \mathrm{J2R}^2} - 2\,\sigma.\mathrm{K4I}.\mathrm{K3R}.\mathrm{SS}\sqrt{\mathrm{J2I}^2 + \mathrm{J2R}^2}$

$$B = -\left[4\,\sigma^2\mathrm{K5I}^2 + 4\,\sigma^2\mathrm{K5R}^2 - 8\,\sigma^3\mathrm{K3I} + 8\mathrm{CS}.\ \sigma^2.\mathrm{K4I}\sqrt{\mathrm{J2I}^2 + \mathrm{J2R}^2} - 8\ \sigma^2.\mathrm{K4R}.\mathrm{SS}.\sigma\sqrt{\mathrm{J2I}^2 + \mathrm{J2R}^2}\right]$$

$C = 16\,\sigma^4$

The solution of the quartic equation (A14) will produce four roots of αy(T1):

$$\alpha y(T1) = \pm\sqrt{-\frac{\left(B - \sqrt{B^2 - 4AC}\right)}{2A}} \quad or \quad \alpha y(T1) = \pm\sqrt{-\frac{\left(B + \sqrt{B^2 - 4AC}\right)}{2A}} \qquad (131)$$

However, the acceptable solution for αy(T1) is the root of the quartic equation (115) that is real and positive [25-27].

Peer-reviewed version available at Math. Comput. Appl. 2017, 22, 44; doi:10.3390/mca22040044

REFERENCES

[1].S. Miwa, M. Mori and T. Hibiki, "Two-phase flow induced vibration in piping systems" Progress in Nuclear Energy 78 (2015) 270–284.

[2].C. Monette and M.J. Pettigrew, "Fluidelastic instability of flexible tubes subjected to two –phase internal flow" Journal of Fluids and Structures 19 (2004) 943–956.

[3].C. Semler, G.X. Li and M.P. Païdoussis, "The Nonlinear Equations of Motion of Pipes Conveying Fluid" Journal of Sound and Vibration 169 (1994) 577–599.

[4].R.W. Gregory and M.P. Païdoussis, "Unstable oscillation of tubular cantilevers conveying fluid. I. Theory" Proceedings of the Royal Society of London. Series A. Mathematical and Physical Sciences 293 (1966) 512–527.

[5].R. Shilling and Y. K. Lou, "An Experimental Study on the Dynamic Response of a Vertical Cantilever Pipe Conveying Fluid" Journal of Energy Resource Technology 102(3) (1980) 129–135.

[6].M.H. Ghayesh, M.P. Païdoussis and M. Amabili, "Nonlinear dynamics of cantilevered extensible pipes conveying fluid" Journal of Sound and Vibration 332 (2013) 6405–6418.

[7].J. Łuczko, A. Czerwiński, "Parametric vibrations of pipes induced by pulsating flows in hydraulic systems" journal of theoretical and applied mechanics 52(3) (2014) 719–730.

[8].M.P. Païdoussis, "Fluid-Structure Interactions: Slender Structures and Axial Flow" vol. 1, Elsevier Academic Press, London, ISBN- 9780125443616 (2003).

[9].Y.M. Sadeghi and M.P. Païdoussis, "Nonlinear Dynamics of Extensible Fluid-Conveying Pipes, Supported at Both Ends" Journal of Fluids Structures 25(3) (2009) 535–543.

[10].L. Wang H.L. Dai, Q. Qian, "Dynamics of simply supported fluid-conveying pipes with geometric imperfections" Journal of Fluids Structures, 29 (2012) 97–106.

[11].B.G. SINIR, "Bifurcation and chaos of slightly curved pipes", Mathematical and Computational Applications, 15 (3) (2010) 490–502.

[12].T.G. Ritto, C. Soize, F.A. Rochinha, R. Sampaio "Dynamic stability of a pipe conveying fluid with an uncertain computational model". Journal of Fluids Structures 49 (2014) 412–426.

[13].L.Q. Chen, Y.L. Zhang, G.C. Zhang, H. Ding "Evolution of the double-jumping in pipes conveying fluid flowing at the supercritical speed" International Journal of Non-Linear Mechanics 58 (2014) 11–21.

[14].A.H. Nayfeh, "Finite Amplitude Longitudinal Waves in Non-uniform Bars" Journal of Sound and Vibrations 42(3) (1975) 357–361.

[15].A.H. Nayfeh, "Perturbation Methods" Wiley-VCH Verlag GmbH & Co. KGaA, Weinheim, ISBN 9780471399179 (2004).

[16].A. Kesimli, S.M. Bağdatlı and S. Çanakcı, "Free vibrations of fluid conveying pipe with intermediate support" Research on Engineering Structures and Materials 2(2) (2016) 75–87.

[17].H.R. Oz and H. Boyaci, "Transverse vibrations of tensioned pipes conveying fluid with time-dependent velocity" Journal of Sound and Vibration 236(3) (2000) 259–276.

[18].S. EnZ, "Effect of asymmetric actuator and detector position on Coriolis flowmeter and measured phase shift. Flow Measurement and Instrumentation" 21 (2010) 497–503.

[19].H.R. Oz and M. Pakdemirli, "Vibrations of an axially moving beam with time-dependent velocity" Journal of Sound and Vibration 227(3) (1999) 239–257.

[20].B.G. Sinir and D.D. Demir, "The analysis of nonlinear vibrations of pipe conveying ideal fluid" European Journal of Mechanics B/Fluids 52 (2015) 38–44.

[21].J.J. Thomsen, "Vibrations and Stability" Springer, ISBN 3540401407 (2003).

[22].A.H. Nayfeh and D.T. Mook, "Nonlinear Oscillations" John Wiley and sons, Inc. ISBN 0471121428 (1995).

[23].Y.M. Sadaghi, M.P. Paidoussis, and C. Semler, "A nonlinear model for an extensible slender flexible cylinder subjected to axial flow" Journal of Fluids and Structures 21 (2005) 609–627.

[24].M.A. Woldesemayat and A.J Ghajar, "Comparison of void fraction correlations for different flow patterns in horizontal and upward inclined pipes" International Journal of Multiphase Flow 33 (2007) 347–370.

[25].S.S. Oueini, C.M. Chin and A.H. Nayfeh, "Dynamics of Cubic Nonlinear Vibration Absorber" Nonlinear Dynamics 20 (1999) 283–295.

[26].H. Jo and H. Yabuno, "Amplitude reduction of parametric resonance by dynamic vibration absorber on quadratic nonlinear coupling" Journal of Sound and Vibration 329 (2010) 2205–2217.

[27].E.L. Rees, "General Discussion of the Roots of a Quartic Equation" The American Mathematical Monthly 29(2) (1922) 51–55.